Appendix

A. The Definition of Demographic Categories

Skin Tone: Skin tone is an important attribute of human appearance, with significant variation from pale to dark. Recently, AI systems, especially computer vision models, have become controversial over concerns about the potential bias of performance varying based on skin tone [46, 106, 107]. Additionally, existing research has pointed out that skin tone annotations can be potentially less biased than building a racial classifier [108]. And the ethnicity attribute is subjective and can conceptually cause confusion in many aspects; for example, there may be no difference in facial appearance of African-American and African people, although, they may be referred to with two distinct racial categories. We, therefore, have opted to annotate the apparent skin tone of each face image. The Monk Skin Tone Scale [48] is developed specifically for the computer vision use case. We intentionally use the Monk Skin Tone scale over the Fitzpatrick skin type [109], which is developed as means for determining one's likelihood of getting sunburn and lacks variance in darker skin tones [110, 111]. Additionally, Fitzpatrick skin type has been shown to be unreliable for image annotation [112].

Gender: Many governments [49, 50] have adopted binary gender (*i.e*., Man/Male (M) and Woman/Female(F), defined as sex at birth, as a common choice for legal and institutional systems and official documents. Most facial recognition research [45, 51, 52] also considers binary genders in their analyses. Our AI-Face dataset adopts binary gender as gender attributes.

Age: Follow United Nations [53] and Statistics Canada [54], we have five distinct perceived age groups- Child (0-14), Youth (15-24), Adults (25-44), Middle-age Adults (45-64), and Seniors (65+).

The demographic attribute and its corresponding example images are shown from Fig. A.1 to Fig. A.3.

B. The Details of Demographically Annotated AI-Face Dataset

B.1. Detailed Information of Datasets

We build our AI-Face dataset by collecting and integrating public real and AI-generated face images sourced from academic publications, GitHub repositories, and commercial tools. We strictly adhere to the license agreements of all datasets to ensure that they allow inclusion in our datasets and secondary use for training and testing. Table B.1 shows the detailed information of each dataset we used in our AI-Face, including the number of samples, the link for downloading the dataset, the accessibility, and their licenses.

B.2. Artifacts of Deepfake Forgeries in Frequency

Leveraging frequency domain information plays a pivotal role in detecting AI-generated images. Frequency-based methods analyze the frequency components of an image, capturing information that may not be readily apparent in the spatial domain. In Fig. B.2, we present the mean Fast Fourier Transform (FFT) spectrum of images sampled from various sources in our AI-Face dataset. The results indicate that generative models often concentrate their output energy in the low-frequency range, represented by the central area of the FFT spectrum, resulting in overly smooth images. Notably, some models, such as StarGAN and Midjourney, exhibit distinct frequency artifacts, suggesting that they continue to struggle with eliminating generative patterns in the frequency domain. These artifacts serve as critical cues for distinguishing synthetic images from real ones. While most prior work has focused on applying frequency information to enhance the utility performance of detectors, exploring how frequency features can be leveraged to improve the fairness of detectors presents a promising direction for future research.

B.3. Experimental Study of Existing Face Attribute Prediction Tools

We compare current state-of-the-art face attribute prediction tools Face++ [71] and InsightFace [72] with our annotator. We perform *intra-domain* (train and test on IMDB-WIKI) and *cross-domain* (train on IMDB-WIKI, test on four AI-generated face datasets) evaluations. FF++, DFDC, DFD, and Celeb-DF-v2 are selected for cross-domain evaluation because they contain AI-generated faces, which match our objective and are not used to train Face++ and InsightFace. Additionally, they have demographic attribute annotations from [19], which can be used as ground truth for annotator evaluation. Since those annotations provided by [19] have limited age annotations, our evaluation of these four datasets is confined to gender. The intra-domain results are shown in Table B.2 and the results of cross-domain are in Table B.3. Those results demonstrate our annotator's superiority in demographic attribute prediction and generalization capability against Face++ and InsightFace. For example, under intra-domain evaluation (Table B.2), its precision surpasses the second-best method, InsightFace, by 3.47% on

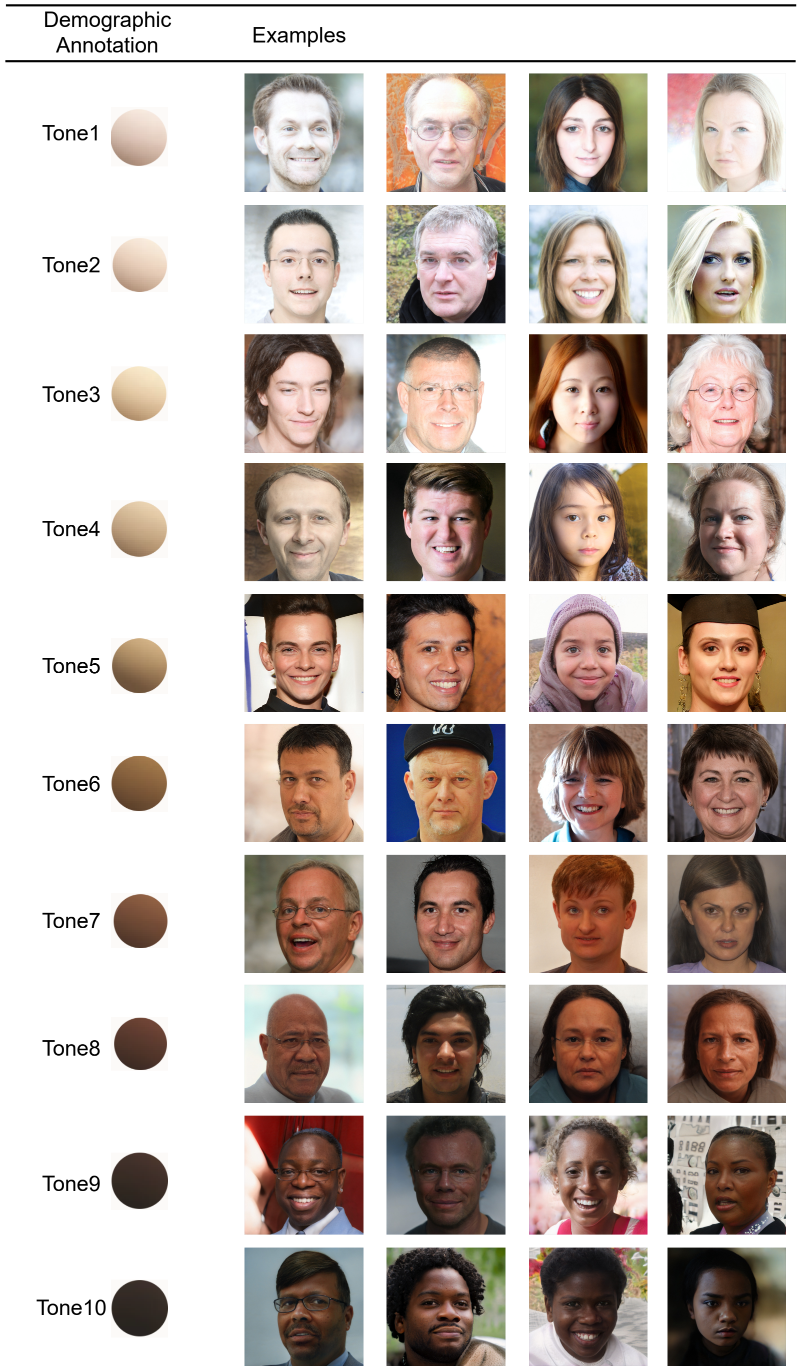

Figure A.1. *Demographic annotation definition and examples of **skin tone** attribute.*

Female and 24.81% on Senior. In cross-domain evaluation (Table B.2), our annotator maintains high accuracy on all datasets, reflecting good generalization. For instance, on the DFDC dataset, the precision our annotator outperforms Face++ by a margin of up to 1.07% and InsightFace by 3.32% on Female.

B.4. Annotator Implementation Detail

Our annotators are implemented by PyTorch and trained with a single NVIDIA RTX A6000 GPU. For training, we fix the batch size 64, epochs 32, and use Adam optimizer with an initial learning rate $\beta = 1e-3$. Additionally, we employ a

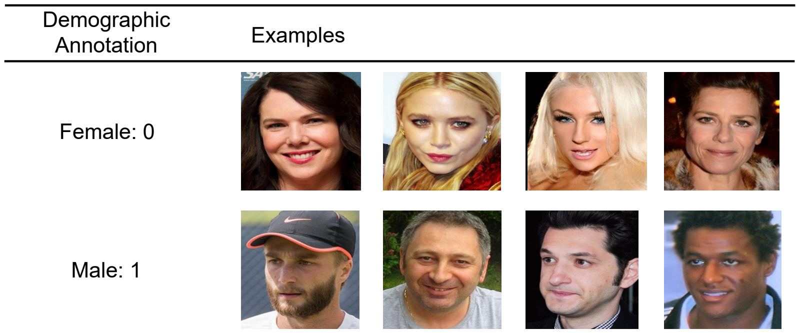

Figure A.2. *Demographic annotation definition and examples of* ***gender*** *attribute.*

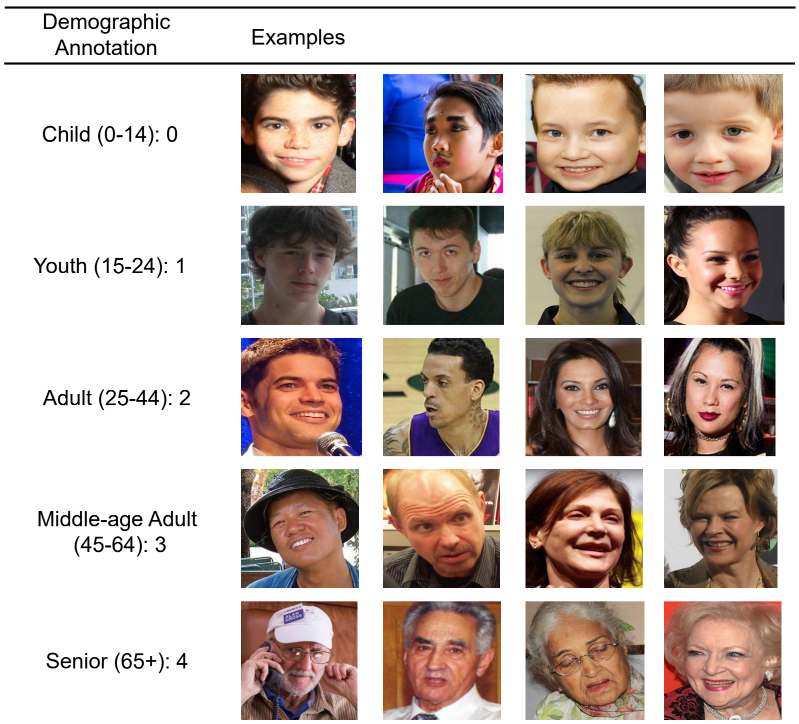

Figure A.3. *Demographic annotation definition and examples of* ***age*** *attribute.*

Cosine Annealing Learning Rate Scheduler to modulate the learning rate adaptively across the training duration. In terms of the imbalance loss, u_{A_i} is the weighting factor for attribute A_i. $h(f_i)_{A_i}$ is the predict logit on A_i. ζ_{A_i} is the multiplicative logit scaling factor, $\zeta_{A_i} = \left(\frac{N_{A_i}}{N_{\text{max}}}\right)^{\kappa}$, N_{max} is the number of samples in the most frequent class, κ is the hyperparameter controlling the sensitivity of scaling, it is set as 0.2 here. Δ_{A_i} is the additive logit scaling factor, calculated as the log of A_i probabilities $\Delta_{A_i} = \rho \cdot \log\left(\frac{N_{A_i}}{N_{\text{total}}}\right)$. The regularization hyperparameter α in fairness loss is 1e-4. The hyperparameter γ in SAM optimization is set as 0.05.

B.5. Details of Human Labeling Activities in Annotation Quality Assessment

The annotation process for assessing the quality of AI-generated face image annotations followed a structured and ethically grounded methodology. Prior to labeling, all human annotators signed an Annotator Agreement E.9 outlining the project objectives, confidentiality requirements, and detailed labeling guidelines for gender and age classification. This agreement emphasized impartiality, respect, and adherence to professional conduct throughout the annotation activities. Human annotators then underwent tutorial training using real example images to familiarize themselves with demographic attributes and labeling criteria, focusing on identifying gender-specific features, such as facial structure and presence of facial hair, and age-related

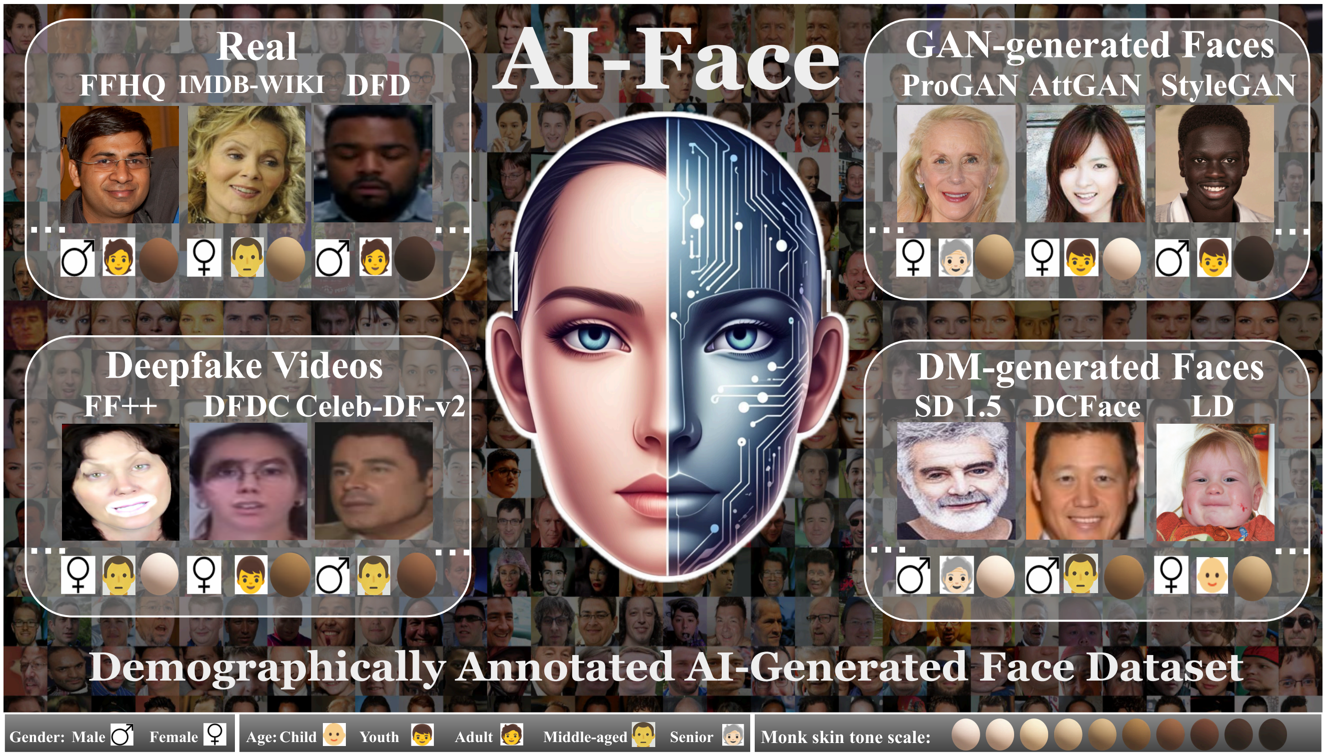

Figure B.1. *Overview of AI-Face dataset. Each face has three demographic annotations.*

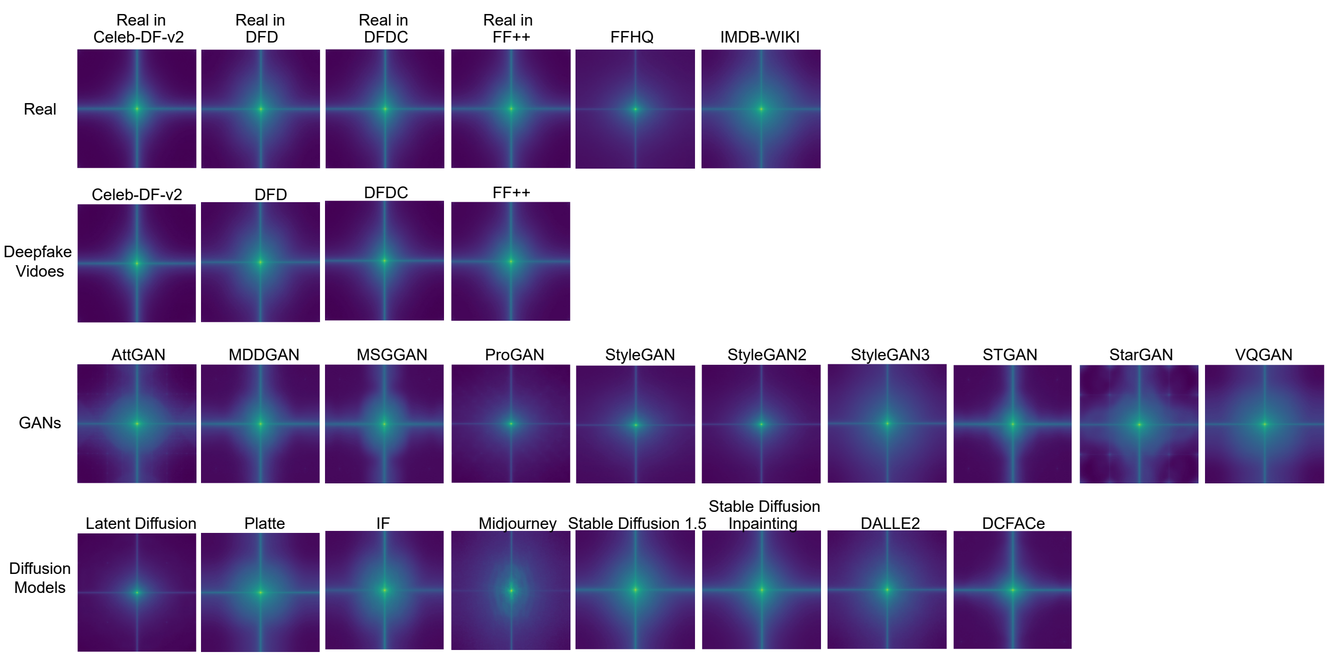

Figure B.2. *Frequency analysis on various sources. The mean FFT spectrum computation involves averaging over 2,000 images. DALLE2, IF, and Midjourney take average over 200, 500, and 100, respectively, due to their small number of samples.*

indicators, including wrinkles and skin elasticity.

Following the agreement and training, human annotators independently labeled the images based on the established criteria,

Dataset	#Samples	Link	Access	License
FF++ [2]	127K	https://github.com/ondyari/FaceForensics/tree/master/dataset	freely shared for a research purpose, submit aggreement	Non Commercial
DFDC [21]	75K	https://www.kaggle.com/c/deepfake-detection-challenge/data	the rights have been cleared for real videos, submit aggreement	Unknown
DFD [22]	40K	https://research.google/blog/contributing-data-to-deepfake-detection-research/		Non Commercial
Celeb-DF-v2 [23]	179K	https://cse.buffalo.edu/$\sim$siweilyu/celeb-deepfakeforensics.html	freely shared for a research purpose, submit aggreement	Non Commercial
AttGAN [55]	6K	https://iplab.dmi.unict.it/mfs/Deepfakes/PaperGANDCT-2021/	Online dataset, download directly, no license or agreement to sign	Unknown
StarGAN [55]	5.6K			
StyleGAN [55]	10K			
StyleGAN2 [57]	118K	https://github.com/SelfishGene/SFHQ-dataset	Since all images in this dataset are synthetically generated there are no privacy issues or license issues surrounding these images.	MIT License
StyleGAN3 [58]	26.7K	https://huggingface.co/datasets/InfImagine/FakeImageDataset	This dataset are fully open for academic research and can be used for commercial purposes with official written permission.	Apache-2.0
MMDGAN [56]	1K	https://github.com/vishal3477/Reverse_Engineering_GMs/blob/main/dataset/	The dataset can be used for research purposes only and can be used for commercial purposes with official written permission.	Non Commercial
MSGGAN [56]	1K			
STGAN [56]	1K			
ProGAN [59]	100K	https://drive.google.com/drive/folders/1jU-hzyvDZNn_M3ucuvs9xxtJNc9bPLGJ	Online dataset, download directly, no license or agreement to sign	Unknown
VQGAN [60]	50K	https://github.com/awsaf49/artifact	This dataset comes from ArtiFact dataset, which dataset takes leverage of data from multiple methods thus different parts of the dataset come with different licenses.	MIT License
DALLE2 [61]	204	https://github.com/ZhendongWang6/DIRE	freely shared for a research purpose	Unknown
IF [61]	505			
Midjourney [61]	100			
DCFACe [62]	529K	https://github.com/mk-minchul/dcface	freely shared for a research purpose	
Latent Diffusion [63]	20K	https://github.com/grip-unina/DMimageDetection	Copyright 2024 Image Processing Research Group of University Federico II of Naples ('GRIP-UNINA'). All rights reserved.Licensed under the Apache License, Version 2.0 (the "License")	Apache-2.0
Palette [64]	6K	https://github.com/awsaf49/artifact/?tab=readme-ov-file#data-generation	This dataset comes from ArtiFact dataset, which dataset takes leverage of data from multiple methods thus different parts of the dataset come with different licenses.	MIT License
SD v1.5 [65]	18K	https://huggingface.co/datasets/OpenRL/DeepFakeFace	freely shared for a research purpose	Apache-2.0
SD Inpainting [65]	20.9K			
FFHQ [6]	70K	https://github.com/NVlabs/ffhq-dataset	You can use, redistribute, and adapt it for non-commercial purposes, as long as you (a) give appropriate credit by citing our paper, (b) indicate any changes that you've made,and (c) distribute any derivative works under the same license.	Creative Commons BY-NC-SA 4.0 license
IMDB-WIKI [20]	239K	https://data.vision.ee.ethz.ch/cvl/rrothe/imdb-wiki/	This dataset is made available for academic research purpose only. All the images are collected from the Internet, and the copyright belongs to the original owners.	Non Commericial

Table B.1. *A list of datasets used in AI-Face, including the number of samples, links, access details, and licenses.*

Method	Female			Male			Child			Young			Adult			Mid			Senior		
	Precision	Recall	F1	Precision	Recall	F1	Precision	Recall	F1	Precision	Recall	F1	Precision	Recall	F1	Precision	Recall	F1	Precision	Recall	F1
Face ++	0.9161 (0.0064)	0.9142 (0.0031)	0.9151 0.0045	0.9143 (0.0033)	0.9163 (0.0067)	0.9153 0.0048	0.8579 (0.0962)	0.0220 (0.0062)	0.0429 (0.0119)	0.3942 (0.0222)	0.2940 (0.0161)	0.3368 (0.0186)	0.3215 (0.0054)	0.6700 (0.0192)	0.4345 (0.0087)	0.5423 (0.0160)	0.6460 (0.0210)	0.5894 (0.0147)	0.8078 (0.0143)	0.7700 (0.0165)	0.7884 (0.0127)
Insightface	0.9648 (0.0055)	0.9405 (0.0058)	0.9525 0.0017	0.9420 (0.0050)	0.9656 (0.0057)	0.9537 0.0017	**1.0000 (0.0000)**	0.0020 (0.0016)	0.0040 (0.0032)	0.3970 (0.0337)	0.0693 (0.0098)	0.1180 (0.0155)	0.2599 (0.0027)	0.6180 (0.0124)	0.3659 (0.0048)	0.4105 (0.0067)	0.5733 (0.0196)	0.4783 (0.0094)	0.7224 (0.0124)	0.7560 (0.0238)	0.7386 (0.0143)
Ours	**0.9995 (0.0006)**	**0.9992 (0.0006)**	**0.9993 0.0006**	**0.9992 (0.0006)**	**0.9995 (0.0006)**	**0.9993 0.0006**	0.9787 (0.0027)	**0.9780 (0.0062)**	**0.9783 (0.0039)**	**0.9560 (0.0078)**	**0.9393 (0.0080)**	**0.9476 (0.0042)**	**0.9265 (0.0122)**	**0.9547 (0.0107)**	**0.9402 (0.0058)**	**0.9498 (0.0123)**	**0.9320 (0.0123)**	**0.9408 (0.0124)**	**0.9642 (0.0085)**	**0.9700 (0.0087)**	**0.9671 (0.0082)**

Table B.2. *Detailed comparison of our annotator against Face++ [71] and InsightFace [72] on IMDB-WIKI [20] dataset. Prediction mean and standard deviation (in parentheses) of each method across 5 random samplings are reported. The best results are shown in Bold.*

categorizing gender and age into predefined classes, and recorded their annotations in a CSV file. A structured conflict resolution approach ensured accuracy and consistency in annotations. Labels agreed upon by a majority of annotators were finalized directly, while unanimous disagreements were resolved through collaborative discussions guided by the annotation guidelines. This process ensured that all annotations were objective, reliable, and aligned with ethical standards set forth in the signed agreement.

Dataset	Method	Female precision	Female recall	Female F1	Male precision	Male recall	Male F1
FF++	Face ++	**0.9816** **(0.3021)**	0.9795 (0.1360)	0.9805 (0.1459)	0.9795 (0.1312)	**0.9816** **(0.3084)**	0.9805 (0.1508)
	Insightface	0.9700 (0.4697)	0.9664 (0.6046)	0.9682 (0.3867)	0.9666 (0.5794)	0.9713 (0.4815)	0.9683 (0.3802)
	Ours	0.9799 (0.0022)	**0.9992** **(0.0006)**	**0.9894** **(0.0009)**	**0.9992** **(0.0007)**	0.9795 (0.0023)	**0.9892** **(0.0009)**
DFDC	Face ++	0.9412 (0.9771)	0.8992 (1.0095)	0.9197 (0.5639)	0.9035 (0.8353)	0.9437 (1.0246)	**0.9231** **(0.5353)**
	Insightface	0.9187 (0.9855)	0.7869 (1.7976)	0.8475 (0.7444)	0.8139 (1.1401)	0.9301 (1.0587)	0.8680 (0.3842)
	Ours	**0.9519** **(0.0106)**	**0.9741** **(0.0014)**	**0.9629** **(0.0059)**	**0.9735** **(0.0015)**	**0.9507** **(0.9619)**	0.0114 (0.0064)
DFD	Face ++	**0.9501** **(0.3773)**	0.8228 (1.8758)	0.8818 (1.0113)	0.8440 (1.3784)	**0.9568** **(0.3907)**	0.8968 (0.6856)
	Insightface	0.9441 (0.7765)	0.7557 (0.9555)	0.8394 (0.7937)	0.7964 (0.6834)	0.9552 (0.6344)	0.8686 (0.5961)
	Ours	0.9378 (0.0045)	**0.9365** **(0.0053)**	**0.9366** **(0.0033)**	**0.9366** **(0.0049)**	0.9379 (0.0048)	**0.9372** **(0.0033)**
Celeb-DF-v2	Face ++	0.9989 (0.0553)	0.9648 (0.4182)	0.9815 (0.2361)	0.9660 (0.3918)	0.9989 (0.0533)	0.9822 (0.2215)
	Insightface	0.9984 (0.0541)	0.9811 (0.3518)	0.9896 (0.1801)	0.9814 (0.3396)	0.9984 (0.0534)	0.9898 (0.1737)
	Ours	**1.0000** **(0.0000)**	**0.9997** **(0.0005)**	**0.9999** **(0.0003)**	**0.9997** **(0.0005)**	**1.0000** **(0.0000)**	**0.9999** **(0.0003)**

Table B.3. *Detailed comparison of our annotator against Face++ [71] and InsightFace [72] on FF++ [2], DFDC [21], DFD [22], and Celeb-DF-v2 [23] datasets. Prediction mean and standard deviation (in parentheses) of each method across 5 random samplings. The best results are shown in Bold.*

B.6. Visualization of Skin Tone Annotation Generation

The visualization shown in Fig. B.3 illustrates the skin tone estimation process using the Monk Skin Tone (MST) Scale. Each row represents a sample image, showing the progression from the original face with facial landmarks to the masked skin region that excludes non-skin areas like eyes and lips. Subsequently, the K-Means clustered skin region highlights the dominant skin tones extracted from the facial area. On the right, bar plots display the proportions of the top three dominant tones within the clustered region, with the top tone (largest cluster) mapped to the closest MST Scale shade. This mapping is achieved by calculating the maximum similarity, as indicated by the Euclidean distance in RGB space between the cluster centroid and MST reference colors. This process visually demonstrates how the methodology isolates, clusters, and estimates skin tones for accurate skin tone annotation generation.

C. Fairness Benchmark Settings

C.1. Implementation Detail

For fairness benchmark, all experiments are based on the PyTorch with a single NVIDIA RTX A6000 GPU. During training, we utilize SGD optimizer with a learning rate of 0.0005, with momentum of 0.9 and weight decay of 0.005. The batch size is set to 128 for most detectors. However, for the SRM [87], UCF [26], and PG-FDD [30], the batch size is adjusted to 32 due to GPU memory. For hyperparameters defined in these detectors, we use the default values set in their original papers. All detectors are initialized with their official pre-trained weights, and trained for 10 epochs.

C.2. Details of Detection Methods

We summarized the backbone architecture, GitHub repository link, and publication venue of the detectors implemented in our fairness benchmark in Table C.1. A brief introduction to each detector is provided below:

Xception [82]: is a deep convolutional neural network (CNN) architecture that relies on depthwise separable convolutions. This approach significantly reduces the number of parameters and computational cost while maintaining high performance. Xception serves as a classic backbone in deepfake detectors.
EfficientB4 [83]: is part of the EfficientNet family [83], which utilizes a novel model scaling method that uniformly scales all

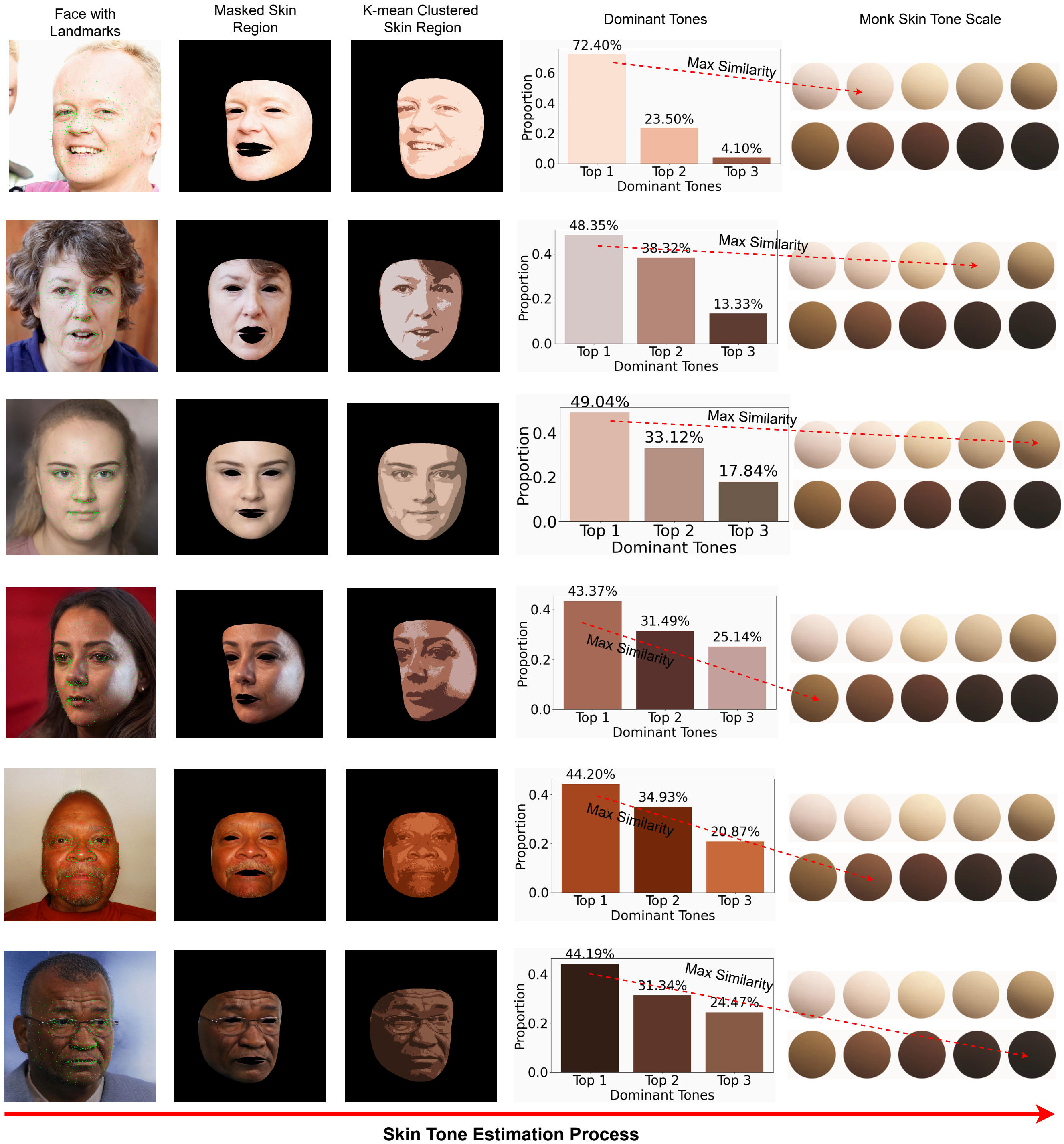

Figure B.3. *Visualization of the skin tone estimation process.*

dimensions of depth, width, and resolution using a compound coefficient. EfficientNet also serves as a classic backbone in deepfake detectors.

ViT-B/16 [84]: is a model that applies the transformer architecture, the 'B' denotes the base model size, and '16' indicates the patch size. ViT-B/16 splits images into 16 patches, linearly embeds each patch, adds positional embeddings, and feeds the resulting sequence of vectors into a standard transformer encoder.

Model Type	Detector	Backbone	GitHub Link	VENUE
Naive	Xception [82]	Xception	https://github.com/ondyari/FaceForensics/blob/master	ICCV-2019
	Efficient-B4 [83]	EfficientNet	https://github.com/lukemelas/EfficientNet-PyTorch	ICML-2019
	ViT-B/16 [84]	Transformer	https://github.com/lucidrains/vit-pytorch	ICLR-2021
Spatial	UCF [26]	Xception	https://github.com/SCLBD/DeepfakeBench/tree/main	ICCV-2023
	UnivFD [88]	CLIP VIT	https://github.com/Yuheng-Li/UniversalFakeDetect	CVPR-2023
	CORE [89]	Xception	https://github.com/niyunsheng/CORE	CVPRW-2022
Frequency	F3Net [85]	Xception	https://github.com/yyk-wew/F3Net	ECCV-2020
	SRM [87]	Xception	https://github.com/SCLBD/DeepfakeBench/tree/main	CVPR-2021
	SPSL [86]	Xception	https://github.com/SCLBD/DeepfakeBench/tree/main	CVPR-2021
Fairness-enhanced	DAW-FDD [29]	Xception	Unpublished code, reproduced by us	WACV-2024
	DAG-FDD [29]	Xception	Unpublished code, reproduced by us	WACV-2024
	PG-FDD [30]	Xception	https://github.com/Purdue-M2/Fairness-Generalization	CVPR-2024

Table C.1. *Summary of the implemented detectors in our fairness benchmark.*

F3Net [85]: utilizes a cross-attention two-stream network to effectively identify frequency-aware clues by integrating two branches: FAD and LFS. The FAD (Frequency-aware Decomposition) module divides the input image into various frequency bands using learnable partitions, representing the image with frequency-aware components to detect forgery patterns through this decomposition. Meanwhile, the LFS (Localized Frequency Statistics) module captures local frequency statistics to highlight statistical differences between authentic and counterfeit faces.

SPSL [86]: integrates spatial image data with the phase spectrum to detect up-sampling artifacts in face forgeries, enhancing the model's generalization ability for face forgery detection. The paper provides a theoretical analysis of the effectiveness of using the phase spectrum. Additionally, it highlights that local texture information is more important than high-level semantic information for accurately detecting face forgeries.

SRM [87]: extracts high-frequency noise features and combines two different representations from the RGB and frequency domains to enhance the model's generalization ability for face forgery detection.

UCF [26]: presents a multi-task disentanglement framework designed to tackle two key challenges in deepfake detection: overfitting to irrelevant features and overfitting to method-specific textures. By identifying and leveraging common features, this framework aims to improve the model's generalization ability.

UnivFD [88]: uses the frozen CLIP ViT-L/14 [73] as feature extractor and trains the last linear layer to classify fake and real images.

CORE [89]: explicitly enforces the consistency of different representations. It first captures various representations through different augmentations and then regularizes the cosine distance between these representations to enhance their consistency.

DAW-FDD [29]: a demographic-aware Fair Deepfake Detection (DAW-FDD) method leverages demographic information and employs an existing fairness risk measure [113]. At a high level, DAW-FDD aims to ensure that the losses achieved by different user-specified groups of interest (*e.g.*, different races or genders) are similar to each other (so that the AI face detector is not more accurate on one group vs another) and, moreover, that the losses across all groups are low. Specifically, DAW-FDD uses a CVaR [114, 115] loss function across groups (to address imbalance in demographic groups) and, per group, DAW-FDD uses another CVaR loss function (to address imbalance in real vs AI-generated training examples).

DAG-FDD [29]: a demographic-agnostic Fair Deepfake Detection (DAG-FDD) method, which is based on the distributionally robust optimization (DRO) [116, 117]. To use DAG-FDD, the user does not have to specify which attributes to treat as sensitive such as race and gender, only need to specify a probability threshold for a minority group without explicitly identifying all possible groups.

PG-FDD [30]: PG-FDD (Preserving Generalization Fair Deepfake Detection) employs disentanglement learning to extract demographic and domain-agnostic forgery features, promoting fair learning across a flattened loss landscape. Its framework combines disentanglement learning, fairness learning, and optimization modules. The disentanglement module introduces a loss to expose demographic and domain-agnostic features that enhance fairness generalization. The fairness learning module combines these features to promote fair learning, guided by generalization principles. The optimization module flattens the loss landscape, helping the model escape suboptimal solutions and strengthen fairness generalization.

C.3. Fairness Metrics

We assume a test set comprising indices $\{1, \ldots, n\}$. Y_j and $\hat{Y}_j$ respectively represent the true and predicted labels of the sample X_j. Their values are binary, where 0 means real and 1 means fake. For all fairness metrics, a lower value means better performance. The formulations of fairness metrics are as follows,

$$F_{EO} := \sum_{\mathcal{J}_j \in \mathcal{J}} \sum_{q=0}^{1} \left| \frac{\sum_{j=1}^{n} \mathbb{I}_{[\hat{Y}_j=1, D_j=\mathcal{J}_j, Y_j=q]}}{\sum_{j=1}^{n} \mathbb{I}_{[D_j=\mathcal{J}_j, Y_j=q]}} - \frac{\sum_{j=1}^{n} \mathbb{I}_{[\hat{Y}_j=1, Y_j=q]}}{\sum_{j=1}^{n} \mathbb{I}_{[Y_j=q]}} \right|,$$

$$F_{OAE} := \max_{\mathcal{J}_j \in \mathcal{J}} \left\{ \frac{\sum_{j=1}^{n} \mathbb{I}_{[\hat{Y}_j=Y_j, D_j=\mathcal{J}_j]}}{\sum_{j=1}^{n} \mathbb{I}_{[D_j=\mathcal{J}_j]}} - \min_{\mathcal{J}_j' \in \mathcal{J}} \frac{\sum_{j=1}^{n} \mathbb{I}_{[\hat{Y}_j=Y_j, D_j=\mathcal{J}_j']}}{\sum_{j=1}^{n} \mathbb{I}_{[D_j=\mathcal{J}_j']}} \right\},$$

$$F_{DP} := \max_{q \in \{0,1\}} \left\{ \max_{J_j \in \mathcal{J}} \frac{\sum_{j=1}^{n} \mathbb{I}_{[\hat{Y}_j=q, D_j=J_j]}}{\sum_{j=1}^{n} \mathbb{I}_{[D_j=J_j]}} - \min_{J_j' \in \mathcal{J}} \frac{\sum_{j=1}^{n} \mathbb{I}_{[\hat{Y}_j=q, D_j=J_j']}}{\sum_{j=1}^{n} \mathbb{I}_{[D_j=J_j']}} \right\},$$

$$F_{MEO} := \max_{q, q' \in \{0,1\}} \left\{ \max_{J_j \in \mathcal{J}} \frac{\sum_{j=1}^{n} \mathbb{I}_{[\hat{Y}_j=q, Y_j=q', D_j=J_j]}}{\sum_{j=1}^{n} \mathbb{I}_{[D_j=J_j, Y_j=q]}} - \min_{J_j' \in \mathcal{J}} \frac{\sum_{j=1}^{n} \mathbb{I}_{[\hat{Y}_j=q, Y_j=q', D_j=J_j']}}{\sum_{j=1}^{n} \mathbb{I}_{[D_j=J_j', Y_j=q]}} \right\},$$

$$F_{IND} := \sum_{j=1}^{n-1} \sum_{l=j+1}^{n} [|f(X_j) - f(X_l)| - \delta \|X_j - X_l\|_2]_+,$$

where D is the demographic variable, $\mathcal{J}$ is the set of subgroups with each subgroup $\mathcal{J}_j \in \mathcal{J}$. M is the set of detection models and F is the set of fairness metrics. F_{EO} measures the disparity in TPR and FPR between each subgroup and the overall population. F_{OAE} measures the maximum ACC gap across all demographic groups. F_{DP} measures the maximum difference in prediction rates across all demographic groups. And F_{MEO} captures the largest disparity in prediction outcomes (either positive or negative) when comparing different demographic groups. δ in F_{IND} is a predefined scale factor (0.08 in our experiments). $[\cdot]_+$ is the hinge function, $\|\cdot\|_2$ is the ℓ_2 norm. $f(X_j)$ represents the predicted logits of the model for input sample X_j. F_{IND} points that a model should be fair across individuals if similar individuals have similar predicted outcomes.

D. More Fairness Benchmark Results and Analysis

D.1. Detailed Results of Overall Performance Comparison

Detailed test results of each subgroup of each detector on AI-Face are presented in this section. Table D.1 provides comprehensive metrics of each subgroup on AI-Face. These results and findings align with the results reported in Table. 4 submitted main manuscript.

D.2. Performance on Different Age Subgroups

We conduct an analysis of all detectors on age subgroups. **1)** As shown in Fig. D.1, facial images with an age range of 0-14 (Child) are more often misclassified as fake, likely due to the underrepresentation of children in our dataset (see Fig. 3 (b)). This suggests detectors tend to show higher error rates for minority groups and show higher accuracy for the majority (Adult). **2)** Among those detectors, EfficientB4, UnivFD, and PG-FDD demonstrate a smaller FPR gap between age subgroups, indicating these models may be less susceptible to age bias.

D.3. Details of Post-Processing

In Section 4 we have applied 6 post-processing methods to evaluate detectors' robustness. Fig. D.2 visualizes the image after being applied different post-processing methods. We describe each post-processing method as follows:

JPEG Compression: Image compression introduces compression artifacts and reduces the image quality, simulating real-world scenarios where images may be of lower quality or have compression artifacts. In Fig. 6 we apply image compression with quality 80 to each image in the test set.

Gaussian Blur: This post-processing reduces image detail and noise by smoothing it through averaging pixel values with a Gaussian kernel. In Fig. 6 we apply gaussian blur with kernel size 7 to each image in the test set.

Hue Saturation Value: Alters the hue, saturation, and value of the image within specified limits. This post-processing technique is used to simulate variations in color and lighting conditions. Adjusting the hue changes the overall color tone, saturation controls the intensity of colors, and value adjusts the brightness. The results in Fig. 6 are after we adjust hue, saturation, and value with shifting limits 30.

Random Brightness and Contrast: This post-processing method adjusts the brightness and contrast of the image within specified limits. By applying random brightness and contrast variations, it introduces changes in the illumination and contrast

Model Type	Method	Metric	Gender		Skin Tone			Age					Intersection					
			M	F	L	M	D	Child	Young	Adult	Middle	Senior	M-L	M-M	M-D	F-L	F-M	F-D
Naive	Xception [82]	AUC	98.90	98.20	97.69	98.44	98.88	95.95	97.86	99.10	98.66	96.54	97.88	98.70	99.22	97.53	98.17	98.19
		FPR	11.12	15.10	18.37	14.72	9.54	36.83	18.26	8.95	12.78	20.42	17.70	12.82	8.42	18.93	16.58	11.32
		TPR	99.38	99.22	98.94	99.62	98.43	99.55	99.38	99.21	99.49	98.51	98.55	99.64	98.87	99.16	99.59	97.58
		ACC	96.77	95.80	95.16	96.43	96.03	89.83	94.98	97.10	97.06	92.06	94.26	96.79	96.78	95.70	96.10	94.67
	EfficientB4 [83]	AUC	98.86	98.31	99.23	98.94	97.59	99.63	98.61	98.44	98.82	98.69	99.01	99.10	98.36	99.39	98.78	95.94
		FPR	17.57	22.96	21.32	17.17	25.47	16.13	22.92	19.79	19.41	19.07	20.50	15.44	20.74	22.00	18.87	33.02
		TPR	99.04	98.56	99.49	99.02	98.19	99.56	98.89	98.55	99.14	98.66	99.22	99.25	98.60	99.64	98.81	97.40
		ACC	94.91	93.42	94.95	95.43	91.05	95.37	93.45	93.81	95.48	92.62	94.01	95.90	93.04	95.51	94.99	87.44
	ViT-B/16 [84]	AUC	99.02	98.26	97.50	98.77	98.49	95.55	98.23	98.98	98.80	97.28	97.21	99.03	99.03	97.80	98.50	97.21
		FPR	14.06	19.17	21.74	16.86	15.48	28.28	21.09	13.34	17.22	20.92	21.43	14.93	12.61	22.00	18.76	20.05
		TPR	98.43	97.51	96.75	98.23	97.36	94.58	97.88	98.14	98.40	96.16	96.77	98.56	98.21	96.74	97.93	95.72
		ACC	95.33	93.52	92.72	94.88	93.49	88.48	93.16	95.17	95.31	90.34	91.96	95.48	95.10	93.16	94.33	90.55
Frequency	F3Net [85]	AUC	99.09	98.24	98.51	98.68	98.79	96.05	98.17	99.15	98.97	97.40	98.66	99.00	99.27	98.30	98.36	97.80
		FPR	12.49	17.21	30.72	16.54	10.78	49.32	21.21	10.51	12.52	20.00	30.75	14.33	9.38	30.69	18.72	13.02
		TPR	99.15	99.00	99.69	99.41	98.11	99.77	99.40	99.00	99.06	97.96	99.55	99.34	98.76	99.76	99.48	96.86
		ACC	96.25	95.12	93.05	95.87	95.43	86.66	94.27	96.54	96.77	91.84	91.55	96.22	96.42	93.95	95.55	93.63
	SPSL [86]	AUC	98.88	98.58	98.99	98.70	98.81	97.41	98.05	99.17	98.75	97.32	99.05	98.78	99.02	98.92	98.61	98.36
		FPR	11.62	16.03	19.50	14.77	11.44	37.20	20.20	9.58	13.12	19.07	18.94	12.88	9.57	19.95	16.62	14.43
		TPR	99.64	99.52	99.53	99.73	99.15	99.78	99.58	99.53	99.69	99.12	99.44	99.77	99.37	99.58	99.70	98.73
		ACC	96.84	95.80	95.38	96.51	95.96	89.90	94.65	97.17	97.16	92.92	94.59	96.88	96.80	95.85	96.17	94.42
	SRM [87]	AUC	98.45	97.40	98.71	97.94	97.95	97.24	97.27	98.42	98.13	97.78	99.24	98.46	98.52	98.36	97.48	96.82
		FPR	12.84	19.11	22.30	17.50	12.30	36.76	22.42	11.92	15.33	19.64	18.94	14.70	9.92	25.06	20.25	16.10
		TPR	98.84	98.33	99.41	99.02	97.35	99.23	98.91	98.29	98.97	97.52	99.89	99.20	98.06	99.16	98.85	95.99
		ACC	95.93	94.16	94.67	95.35	94.44	89.62	93.59	95.65	96.14	91.67	94.91	96.03	95.76	94.53	94.72	92.03
Spatial	UCF [26]	AUC	98.62	97.45	97.20	97.92	98.49	95.59	97.26	98.74	98.67	97.04	97.67	98.44	99.00	96.88	97.41	97.47
		FPR	11.30	16.37	26.23	16.01	8.90	55.93	21.10	8.43	11.70	20.40	24.85	13.82	7.23	27.37	18.16	11.57
		TPR	98.20	97.77	98.75	98.37	96.89	99.53	98.50	97.58	98.35	96.91	99.00	98.47	97.63	98.61	98.28	95.45
		ACC	95.84	94.39	93.30	95.18	95.14	84.71	93.61	96.03	96.36	91.01	92.70	95.66	96.24	93.65	94.73	93.15
	UnivFD [88]	AUC	98.55	97.76	98.38	98.47	97.40	98.13	98.07	98.33	98.11	96.94	98.24	98.76	98.13	98.46	98.19	95.84
		FPR	16.46	20.97	20.06	19.04	17.60	19.90	19.91	16.70	22.13	17.04	17.70	16.84	15.88	22.00	21.20	20.36
		TPR	98.02	97.12	97.57	98.26	95.69	97.43	97.40	97.39	98.41	94.49	97.10	98.54	96.99	97.83	98.02	93.17
		ACC	94.42	92.80	93.73	94.43	91.68	92.80	93.09	93.74	94.35	90.56	93.19	95.03	93.29	94.04	93.87	88.74
	CORE [89]	AUC	99.04	98.01	97.80	98.47	98.79	95.88	97.82	99.09	98.77	97.11	98.12	98.91	99.26	97.57	98.02	97.84
		FPR	10.73	16.52	21.46	14.76	10.68	43.07	19.42	9.19	12.34	20.10	18.63	12.14	8.45	23.79	17.34	14.25
		TPR	99.40	99.27	99.61	99.51	98.84	99.83	99.27	99.27	99.46	99.00	99.78	99.53	99.13	99.52	99.49	98.28
		ACC	96.88	95.49	95.01	96.34	95.97	88.37	94.61	97.08	97.13	92.49	94.91	96.87	96.95	95.07	95.85	94.17
Fairness-enhanced	DAW-FDD [29]	AUC	98.36	97.15	96.84	97.45	98.51	94.97	96.41	98.62	98.00	94.95	96.83	98.05	98.85	96.77	96.87	97.91
		FPR	14.12	19.63	26.93	18.59	12.81	56.69	23.64	11.23	15.40	26.17	26.40	16.16	10.80	27.37	20.98	16.03
		TPR	99.42	99.24	99.73	99.38	99.20	99.77	99.18	99.28	99.51	98.98	99.78	99.47	99.32	99.70	99.29	98.97
		ACC	96.05	94.73	93.91	95.39	95.58	84.69	93.49	96.56	96.56	90.41	92.86	95.90	96.41	94.53	94.91	94.06
	DAG-FDD [29]	AUC	99.05	98.44	97.56	98.79	98.73	96.55	98.14	99.10	98.91	97.59	98.11	99.00	99.16	97.10	98.57	97.83
		FPR	12.11	18.02	20.76	15.10	14.21	26.95	20.01	11.72	14.61	22.40	18.32	13.04	10.58	22.76	17.14	20.00
		TPR	99.21	99.05	98.98	99.25	98.83	97.64	98.92	99.18	99.37	99.13	98.77	99.33	98.98	99.10	99.17	98.54
		ACC	96.39	94.97	94.67	96.06	94.90	91.07	94.20	96.36	96.61	91.79	94.26	96.51	96.23	94.92	95.65	92.47
	PG-FDD [30]	AUC	99.36	98.94	98.94	99.18	99.13	98.83	98.89	99.35	99.27	97.85	98.97	99.35	99.39	98.89	99.02	98.51
		FPR	9.49	12.68	15.29	12.06	8.82	22.77	14.31	7.97	11.64	19.74	13.35	10.90	7.30	16.88	13.20	11.26
		TPR	98.73	98.21	98.63	98.85	97.43	99.11	98.44	98.28	98.87	97.74	98.66	99.02	98.12	98.61	98.69	96.10
		ACC	96.68	95.61	95.59	96.43	95.55	93.27	95.26	96.66	96.79	91.78	95.49	96.75	96.56	95.65	96.12	93.69

Table D.1. *Detailed test results of each subgroup of each detector on the AI-Face. In the Skin Tone groups, 'L' represents Light (Tone 1-3), 'M' is Medium (4-6), 'D' is Dark (Tone 7-10).*

levels of the images. This evaluates detector's robustness to different illumination conditions. The results in Fig. 6 are after we adjust brightness and contrast with shifting limits 0.4.

Random Crop: Resizes the image to a specified size and then randomly crops a portion of it to the target dimensions. This post-processing method is used to evaluate the detector's robustness to variations in the spatial content of the image. The results in Fig. 6 are after we randomly crop the image with target dimension of 244×244.

Rotation: Rotates the image within a specified angle limit. This post-processing method is used to evaluate the detector's robustness to changes in the orientation of objects within the image. The results in Fig. 6 are after we randomly rotate the image within a range of -30 to 30 degrees.

D.4. Additional Fairness Robustness Evaluation Results

Fig. D.3 to Fig. D.7 demonstrate detectors' robustness analysis in more detail as a function of different degrees of post-processing. Overall, ViT-B/16 [84] and UnivFD [88] show stronger robustness to various post-processing methods compared to other detection methods. Fairness-enhanced detectors do not have robustness against post-processing; this would be a direction for future studies to work on. Figure D.3 presents a detailed robustness analysis in terms of utility and fairness under varying degrees of JPEG compression. The utility of all detectors decreases as image quality is reduced. Among the detectors,

Measure	Attribute	Metric	Model Type											
			Native			Frequency			Spatial			Fairness-enhanced		
			Xception [82]	EfficientB4 [83]	ViT-B/16 [84]	F3Net [85]	SPSL [86]	SRM [87]	UCF [26]	UnivFD [88]	CORE [89]	DAW-FDD [29]	DAG-FDD [29]	PG-FDD [30]
Fairness(%)	Skin Tone	F_{MEO}	10.901	4.384	17.219	14.583	9.620	15.508	14.978	2.441	13.135	12.519	12.597	13.965
		F_{DP}	11.274	9.191	10.713	12.739	11.711	11.282	11.549	8.117	11.968	11.179	12.026	11.768
		F_{OAE}	2.434	3.609	2.276	2.232	2.814	1.780	1.950	2.940	1.658	0.878	1.753	1.439
		F_{EO}	0.160	0.093	0.205	0.209	0.156	0.191	0.186	0.034	0.176	0.165	0.176	0.176
	Gender	F_{MEO}	5.475	5.458	8.003	5.749	5.754	5.848	5.575	3.244	4.367	5.186	5.808	4.086
		F_{DP}	1.205	1.412	2.416	1.340	1.445	1.959	1.810	0.781	0.980	1.715	1.470	1.545
		F_{OAE}	2.043	1.800	1.896	2.054	1.969	1.471	1.569	1.413	1.848	1.430	2.012	1.133
		F_{EO}	0.066	0.063	0.083	0.068	0.067	0.062	0.060	0.043	0.056	0.056	0.068	0.044
	Age	F_{MEO}	28.244	7.460	38.521	27.860	24.768	40.542	44.342	8.584	34.156	36.450	35.031	36.197
		F_{DP}	11.228	12.245	12.140	11.395	11.466	14.564	15.856	16.134	13.525	12.256	13.478	12.082
		F_{OAE}	7.138	5.234	10.940	6.933	6.053	11.126	11.481	4.171	8.294	9.192	8.636	8.934
		F_{EO}	0.460	0.175	0.560	0.460	0.410	0.550	0.610	0.191	0.508	0.537	0.524	0.539
	Intersection	F_{MEO}	15.752	10.644	24.460	18.455	15.157	18.381	17.397	5.300	16.257	14.806	15.219	16.517
		F_{DP}	16.943	14.565	13.773	18.071	17.490	14.943	15.612	12.967	17.063	14.802	16.786	15.513
		F_{OAE}	6.805	8.029	5.025	6.658	7.200	3.614	3.532	6.226	5.079	3.314	5.757	2.989
		F_{EO}	0.355	0.307	0.441	0.440	0.366	0.382	0.382	0.178	0.371	0.336	0.399	0.354
Utility(%)	-	AUC	0.968	0.968	0.981	0.966	0.968	0.967	0.977	0.979	0.975	0.970	0.973	0.978
		ACC	0.931	0.922	0.924	0.930	0.929	0.946	0.951	0.933	0.947	0.941	0.941	0.952
		AP	0.987	0.988	0.994	0.986	0.988	0.985	0.991	0.993	0.989	0.987	0.989	0.991
		EER	0.093	0.101	0.082	0.096	0.095	0.076	0.074	0.083	0.076	0.085	0.084	0.072
		FPR	0.205	0.219	0.290	0.199	0.190	0.205	0.163	0.188	0.144	0.186	0.168	0.151

Table D.2. *Detailed fairness and utility evaluation results on 20% training subset.*

Measure	Attribute	Metric	Model Type											
			Native			Frequency			Spatial			Fairness-enhanced		
			Xception [82]	EfficientB4 [83]	ViT-B/16 [84]	F3Net [85]	SPSL [86]	SRM [87]	UCF [26]	UnivFD [88]	CORE [89]	DAW-FDD [29]	DAG-FDD [29]	PG-FDD [30]
Fairness(%)	Skin Tone	F_{MEO}	9.815	4.414	12.194	10.801	9.275	24.037	12.299	2.568	15.734	12.628	10.463	10.982
		F_{DP}	10.080	10.413	9.475	11.137	10.644	12.550	10.632	8.322	11.251	10.157	10.456	10.928
		F_{OAE}	0.122	0.095	0.146	0.154	0.122	0.281	0.150	0.043	0.180	0.154	0.135	0.143
		F_{EO}	1.472	3.796	3.395	2.088	1.631	3.280	1.533	2.898	2.384	1.571	1.323	1.188
	Gender	F_{DP}	5.576	3.592	6.089	5.985	4.368	7.959	4.400	3.438	5.234	5.960	4.797	5.390
		F_{MEO}	1.817	0.822	1.853	1.566	1.227	2.658	1.481	0.797	1.866	2.053	1.458	2.052
		F_{OAE}	1.559	1.622	1.829	1.966	1.595	1.722	1.338	1.507	1.369	1.473	1.530	1.303
		F_{EO}	0.060	0.047	0.067	0.069	0.052	0.080	0.049	0.045	0.055	0.062	0.055	0.055
	Age	F_{MEO}	32.781	9.931	18.050	26.665	33.004	54.967	43.829	7.840	38.202	41.707	34.285	33.582
		F_{DP}	12.161	12.428	14.762	10.954	13.272	16.006	14.243	16.076	13.394	13.661	11.630	12.955
		F_{OAE}	8.535	4.312	6.949	6.831	8.210	14.795	11.248	4.185	9.906	10.841	8.738	8.520
		F_{EO}	0.474	0.235	0.348	0.432	0.470	0.738	0.611	0.179	0.541	0.585	0.509	0.500
	Intersection	F_{MEO}	13.451	8.558	15.615	13.559	12.356	30.133	15.278	5.585	19.342	17.006	12.784	13.197
		F_{DP}	13.795	16.478	14.409	16.096	15.138	15.893	14.797	13.263	15.123	14.586	14.345	15.166
		F_{OAE}	4.424	7.462	5.221	6.173	4.728	5.030	2.886	6.298	3.741	3.541	4.402	2.911
		F_{EO}	0.312	0.236	0.416	0.360	0.309	0.550	0.304	0.185	0.374	0.324	0.310	0.301
Utility(%)	-	AUC	0.979	0.976	0.980	0.974	0.982	0.957	0.979	0.979	0.981	0.976	0.978	0.982
		ACC	0.951	0.940	0.933	0.937	0.951	0.938	0.955	0.934	0.957	0.948	0.949	0.960
		AP	0.991	0.991	0.993	0.989	0.993	0.983	0.992	0.993	0.991	0.989	0.991	0.992
		EER	0.068	0.078	0.081	0.083	0.066	0.117	0.072	0.082	0.058	0.074	0.074	0.055
		FPR	0.165	0.147	0.136	0.186	0.147	0.245	0.157	0.180	0.151	0.184	0.169	0.130

Table D.3. *Detailed fairness and utility evaluation results on 40% training subset.*

ViT-B/16 [84] exhibits the highest utility robustness, ViT-B/16 [84] and UnivFD [88] both demonstrate the strongest fairness robustness. When considering Gaussian blur, ViT-B/16 again stands out as the most robust detector in terms of utility, whereas DAW-FDD [29] and UnivFD [88] show the great robustness in terms of fairness. Against Hue Saturation Value adjustments, SPSL [86] shows the strongest utility robustness, while the fairness of DAW-FDD [29] fluctuates less with different Hue Saturation Value adjustments. ViT-B/16 demonstrates superior robustness in both utility and fairness when facing rotations. For brightness contrast variations, SPSL [86] is the most robust detector in terms of utility, while UnivFD once again shows superior robustness in terms of fairness. Last, we can get the same conclusion from Fig. D.3 to Fig. D.7 as in the main manuscript, that post-processing clearly impairs detectors' utility but does not necessarily make detectors more biased.

D.5. Full Results of Effect of Increasing the Size of Train Set

In this section, we provide the full evaluation results tested under different sizes of train set, as shown from Table D.2 to Table D.5. Intersection F_{EO} and AUC align with the results in Fig. 7 of the submitted manuscript.

Measure	Attribute	Metric	Model Type											
			Native			Frequency			Spatial			Fairness-enhanced		
			Xception [82]	EfficientB4 [83]	ViT-B/16 [84]	F3Net [85]	SPSL [86]	SRM [87]	UCF [26]	UnivFD [88]	CORE [89]	DAW-FDD [29]	DAG-FDD [29]	PG-FDD [30]
Fairness(%)	Skin Tone	F_{MEO}	9.086	14.704	4.388	15.303	6.813	14.516	14.952	2.186	9.689	13.488	9.672	4.108
		F_{DP}	10.232	11.784	7.714	11.225	9.979	14.909	13.116	8.004	10.666	10.844	10.054	8.575
		F_{OAE}	1.531	2.017	2.572	2.320	1.247	1.733	1.562	2.777	1.208	1.664	1.259	1.383
		F_{EO}	0.124	0.194	0.084	0.177	0.100	0.234	0.208	0.043	0.131	0.163	0.125	0.055
	Gender	F_{MEO}	4.418	6.743	8.445	5.545	5.242	7.331	5.713	4.182	4.395	5.579	4.978	2.430
		F_{DP}	1.243	2.063	2.697	2.096	1.736	3.656	1.845	1.142	1.622	2.153	1.600	1.061
		F_{OAE}	1.567	1.846	2.052	1.318	1.499	0.630	1.651	1.489	1.217	1.267	1.470	0.858
		F_{EO}	0.053	0.072	0.086	0.057	0.057	0.087	0.062	0.050	0.048	0.056	0.055	0.029
	Age	F_{MEO}	35.231	27.998	17.573	42.366	35.428	37.043	34.243	5.520	28.666	40.326	38.409	24.355
		F_{DP}	12.874	12.663	11.691	15.070	12.924	16.570	13.579	15.256	11.264	13.929	13.112	10.449
		F_{OAE}	8.954	7.379	7.004	10.921	8.915	8.078	8.232	3.900	7.519	10.379	9.909	6.870
		F_{EO}	0.514	0.411	0.320	0.585	0.519	0.528	0.520	0.134	0.438	0.570	0.558	0.362
	Intersection	F_{MEO}	11.554	18.923	10.063	18.907	10.175	20.404	18.818	5.414	12.995	15.944	12.552	5.425
		F_{DP}	14.625	15.884	9.908	15.240	14.093	18.967	18.087	12.890	15.331	14.584	13.949	13.379
		F_{OAE}	4.755	4.997	5.459	3.617	4.210	2.965	4.832	6.152	3.747	3.106	4.102	3.306
		F_{EO}	0.279	0.405	0.311	0.362	0.251	0.477	0.431	0.200	0.276	0.331	0.282	0.159
Utility(%)	-	AUC	0.976	0.980	0.986	0.981	0.983	0.976	0.981	0.981	0.982	0.977	0.982	0.982
		ACC	0.948	0.945	0.943	0.961	0.952	0.927	0.951	0.935	0.956	0.960	0.950	0.960
		AP	0.989	0.992	0.996	0.991	0.993	0.991	0.992	0.994	0.992	0.987	0.993	0.991
		EER	0.074	0.071	0.065	0.058	0.067	0.092	0.068	0.078	0.062	0.060	0.069	0.058
		FPR	0.166	0.183	0.177	0.137	0.154	0.137	0.137	0.198	0.145	0.143	0.172	0.127

Table D.4. *Detailed fairness and utility evaluation results on 60% training subset.*

Measure	Attribute	Metric	Model Type											
			Native			Frequency			Spatial			Fairness-enhanced		
			Xception [82]	EfficientB4 [83]	ViT-B/16 [84]	F3Net [85]	SPSL [86]	SRM [87]	UCF [26]	UnivFD [88]	CORE [89]	DAW-FDD [29]	DAG-FDD [29]	PG-FDD [30]
Fairness(%)	Skin Tone	F_{MEO}	15.463	6.826	7.442	13.642	4.221	9.425	13.574	2.368	13.487	10.127	8.763	7.613
		F_{DP}	11.994	10.440	8.378	11.211	8.998	6.875	11.085	8.231	11.506	10.182	8.920	11.914
		F_{OAE}	1.998	2.390	1.540	1.713	2.141	7.511	1.661	2.777	1.538	1.375	1.484	1.822
		F_{EO}	0.192	0.107	0.095	0.171	0.064	0.187	0.168	0.036	0.170	0.119	0.114	0.129
	Gender	F_{MEO}	4.209	3.639	9.461	5.189	4.116	2.328	5.402	4.084	5.058	4.112	4.143	4.035
		F_{DP}	1.171	1.043	3.025	1.749	1.191	2.803	1.778	1.082	1.899	1.537	1.560	1.401
		F_{OAE}	1.579	1.395	2.163	1.499	1.507	1.248	1.560	1.519	1.277	1.218	1.158	1.353
		F_{EO}	0.051	0.045	0.095	0.057	0.050	0.037	0.059	0.050	0.053	0.045	0.045	0.046
	Age	F_{MEO}	33.930	16.272	10.222	45.076	20.048	11.857	45.508	5.788	37.055	30.409	29.707	20.058
		F_{DP}	15.167	11.254	11.643	15.938	11.379	8.360	15.357	15.620	13.565	11.925	9.880	10.487
		F_{OAE}	8.520	4.738	5.662	11.409	5.123	10.447	11.546	3.777	9.454	7.784	8.513	4.450
		F_{EO}	0.488	0.286	0.231	0.623	0.322	0.228	0.625	0.136	0.526	0.441	0.459	0.357
	Intersection	F_{MEO}	19.488	11.396	16.807	15.829	6.631	12.599	16.926	5.116	16.594	13.597	11.226	10.523
		F_{DP}	17.093	15.841	11.946	15.708	13.376	11.010	15.607	13.121	15.834	14.758	12.474	16.906
		F_{OAE}	3.583	5.700	5.469	3.139	5.452	10.020	2.878	6.209	2.852	2.313	2.755	4.348
		F_{EO}	0.392	0.262	0.340	0.349	0.225	0.420	0.342	0.188	0.345	0.254	0.226	0.294
Utility(%)	-	AUC	0.985	0.985	0.987	0.981	0.984	0.979	0.982	0.981	0.984	0.981	0.987	0.988
		ACC	0.950	0.949	0.940	0.958	0.950	0.816	0.956	0.936	0.959	0.963	0.960	0.953
		AP	0.994	0.994	0.996	0.992	0.994	0.992	0.993	0.994	0.993	0.989	0.995	0.996
		EER	0.065	0.064	0.062	0.069	0.064	0.066	0.068	0.078	0.060	0.053	0.057	0.058
		FPR	0.145	0.162	0.206	0.134	0.148	0.039	0.141	0.189	0.138	0.118	0.144	0.099

Table D.5. *Detailed fairness and utility evaluation results on 80% training subset.*

D.6. Full Results of Effect of the Ratio of Real and Fake

In this section, we provide the full evaluation results tested under the train set with different ratios of real and fake, as shown from Table D.6 to Table D.8. Intersection F_{EO} and AUC align with the results in Fig. 7 of the submitted manuscript.

D.7. Comparison Results with Foundation Model

In the Discussion (Section 5.3) of the main manuscript, we highlighted the potential of integrating foundation models (*e.g.*, CLIP) into detector design as a strategy for mitigating bias. To explore this, we conducted a preliminary experiment by designing a detector using a frozen CLIP model combined with a trainable 3-layer MLP. This model was trained and tested on the AI-Face dataset. For comparison, we selected one representative detector from each model type: EfficientB4 [83], SPSL [86], UnivFD [88], and PG-FDD [30]. These four detectors' results are consistent with those reported in Table 4. As shown in Table D.9, the CLIP+MLP detector demonstrates a clear advantage in both fairness and utility metrics, suggesting that foundation models hold significant promise for bias mitigation. For instance, its F_{EO} score is 3.11% lower than the

Measure	Attribute	Metric	Model Type											
			Native			Frequency			Spatial			Fairness-enhanced		
			Xception [82]	EfficientB4 [83]	ViT-B/16 [84]	F3Net [85]	SPSL [86]	SRM [87]	UCF [26]	UnivFD [88]	CORE [89]	DAW-FDD [29]	DAG-FDD [29]	PG-FDD [30]
Fairness(%)	Skin Tone	F_{MEO}	9.750	11.908	5.095	12.896	5.859	18.083	10.363	5.926	10.955	9.570	8.980	3.889
		F_{DP}	16.824	14.637	12.547	17.621	14.479	19.676	15.803	8.744	16.109	16.063	15.700	12.899
		F_{OAE}	2.401	2.973	1.714	3.630	0.905	5.752	3.249	5.302	3.524	2.641	2.684	1.164
		F_{EO}	0.164	0.155	0.119	0.183	0.113	0.248	0.147	0.083	0.149	0.142	0.132	0.069
	Gender	F_{MEO}	3.535	0.952	4.275	4.788	4.439	4.201	4.655	6.898	3.981	3.848	3.674	3.792
		F_{DP}	2.241	0.715	3.129	3.184	3.060	2.245	3.426	4.328	2.850	2.562	2.514	2.790
		F_{OAE}	2.482	0.833	2.263	2.690	2.496	2.920	2.332	3.028	2.236	2.451	2.360	2.166
		F_{EO}	0.051	0.011	0.047	0.057	0.052	0.062	0.049	0.070	0.048	0.051	0.049	0.045
	Age	F_{MEO}	23.282	14.195	13.627	32.679	26.796	52.939	30.332	8.251	32.612	23.934	23.834	15.408
		F_{DP}	17.521	18.304	16.426	20.437	18.489	28.303	18.892	12.343	19.913	17.103	18.221	15.255
		F_{OAE}	11.063	3.474	9.185	16.411	13.102	26.805	15.234	6.602	16.794	11.909	11.523	7.893
		F_{EO}	0.381	0.203	0.303	0.490	0.436	0.769	0.472	0.162	0.469	0.378	0.370	0.273
	Intersection	F_{MEO}	11.921	17.564	7.727	17.622	10.201	21.679	15.031	12.980	12.775	13.010	11.104	7.173
		F_{DP}	23.484	21.311	17.501	23.519	21.115	24.119	22.167	13.434	21.787	22.542	22.120	18.247
		F_{OAE}	4.000	4.650	3.969	5.957	4.306	9.974	5.003	11.530	5.750	3.903	4.600	4.426
		F_{EO}	0.344	0.335	0.304	0.378	0.250	0.515	0.324	0.270	0.325	0.290	0.303	0.196
Utility(%)	-	AUC	0.984	0.984	0.984	0.982	0.982	0.935	0.981	0.979	0.986	0.983	0.987	0.989
		ACC	0.937	0.892	0.922	0.928	0.929	0.900	0.930	0.830	0.933	0.937	0.944	0.940
		AP	0.980	0.986	0.986	0.977	0.978	0.910	0.977	0.980	0.982	0.980	0.984	0.987
		EER	0.062	0.064	0.067	0.061	0.066	0.129	0.065	0.082	0.056	0.061	0.053	0.052
		FPR	0.087	0.005	0.111	0.122	0.111	0.164	0.116	0.337	0.115	0.095	0.083	0.095

Table D.6. *Detailed fairness and utility evaluation results on a training subset with the ratio of real vs fake is 1:1.*

Measure	Attribute	Metric	Model Type											
			Native			Frequency			Spatial			Fairness-enhanced		
			Xception [82]	EfficientB4 [83]	ViT-B/16 [84]	F3Net [85]	SPSL [86]	SRM [87]	UCF [26]	UnivFD [88]	CORE [89]	DAW-FDD [29]	DAG-FDD [29]	PG-FDD [30]
Fairness(%)	Skin Tone	F_{MEO}	11.678	10.565	8.595	12.629	11.790	17.068	9.661	5.615	11.138	11.726	8.680	6.435
		F_{DP}	14.133	12.859	10.579	15.157	13.983	16.962	14.081	8.438	14.161	14.724	13.388	13.256
		F_{OAE}	4.539	3.671	4.407	4.104	4.894	5.036	3.931	5.461	4.389	3.379	3.006	2.232
		F_{EO}	0.128	0.151	0.102	0.148	0.127	0.200	0.107	0.081	0.121	0.141	0.103	0.081
	Gender	F_{MEO}	6.942	2.295	10.586	7.818	7.327	8.990	6.054	6.525	7.518	6.259	5.934	4.944
		F_{DP}	4.378	0.094	6.203	4.881	4.632	5.572	4.086	4.136	4.867	4.093	3.917	3.565
		F_{OAE}	3.225	1.508	4.799	3.669	3.303	4.060	2.906	2.842	3.445	2.890	2.795	2.407
		F_{EO}	0.072	0.023	0.106	0.080	0.074	0.091	0.063	0.067	0.075	0.065	0.062	0.052
	Age	F_{MEO}	36.384	13.175	25.574	35.508	30.942	36.806	32.134	6.629	34.717	32.860	29.474	28.923
		F_{DP}	18.815	19.006	16.522	18.393	17.007	18.947	17.086	12.524	18.454	16.798	15.004	19.634
		F_{OAE}	19.144	2.128	14.899	18.668	16.331	19.294	16.714	6.598	18.249	17.426	15.605	15.099
		F_{EO}	0.524	0.193	0.373	0.525	0.442	0.553	0.490	0.147	0.507	0.482	0.447	0.420
	Intersection	F_{MEO}	16.037	18.196	19.081	16.394	19.895	21.535	13.589	12.135	15.921	14.772	12.424	10.340
		F_{DP}	16.749	17.705	16.207	17.525	18.313	19.312	17.029	12.639	17.144	16.813	15.850	16.846
		F_{OAE}	7.914	4.565	12.301	6.936	8.704	9.372	5.877	11.469	7.025	5.523	6.909	5.109
		F_{EO}	0.381	0.346	0.400	0.399	0.394	0.467	0.317	0.249	0.364	0.336	0.313	0.243
Utility(%)	-	AUC	0.958	0.967	0.975	0.966	0.964	0.951	0.976	0.978	0.969	0.962	0.967	0.983
		ACC	0.864	0.864	0.823	0.876	0.855	0.862	0.909	0.829	0.888	0.874	0.882	0.925
		AP	0.934	0.972	0.976	0.948	0.946	0.938	0.964	0.979	0.952	0.942	0.951	0.977
		EER	0.087	0.098	0.091	0.082	0.081	0.116	0.064	0.085	0.073	0.084	0.079	0.056
		FPR	0.267	0.012	0.349	0.242	0.285	0.272	0.172	0.339	0.221	0.246	0.227	0.142

Table D.7. *Detailed fairness and utility evaluation results on a training subset with the ratio of real vs fake is 1:10.*

second-best method, PG-FDD, for the Skin Tone group, and 14.046% lower for the Intersection group.

Measure	Attribute	Metric	Model Type											
			Native			Frequency			Spatial			Fairness-enhanced		
			Xception [82]	EfficientB4 [83]	ViT-B/16 [84]	F3Net [85]	SPSL [86]	SRM [87]	UCF [26]	UnivFD [88]	CORE [89]	DAW-FDD [29]	DAG-FDD [29]	PG-FDD [30]
Fairness(%)	Skin Tone	F_{MEO}	6.557	11.357	7.743	7.364	5.850	18.290	5.814	12.493	6.397	5.083	6.515	5.122
		F_{DP}	13.087	13.112	12.348	15.751	11.728	22.766	14.881	13.771	14.364	12.265	15.536	12.718
		F_{OAE}	1.779	2.939	1.589	1.352	2.402	3.823	1.495	2.386	0.996	1.401	1.471	1.742
		F_{EO}	0.108	0.140	0.093	0.153	0.090	0.331	0.135	0.155	0.125	0.084	0.143	0.096
	Gender	F_{MEO}	1.808	1.803	2.106	1.659	2.316	3.035	3.035	1.997	3.499	1.920	1.812	3.016
		F_{DP}	1.769	0.136	0.369	1.321	0.470	2.871	2.503	2.008	2.119	1.097	1.405	2.633
		F_{OAE}	1.385	1.269	1.615	1.661	1.777	1.270	1.817	0.579	2.662	1.928	1.734	1.677
		F_{EO}	0.025	0.018	0.027	0.032	0.032	0.038	0.035	0.020	0.052	0.036	0.033	0.033
	Age	F_{MEO}	8.571	11.954	9.832	8.680	9.523	36.509	11.812	10.258	13.180	8.539	9.553	11.109
		F_{DP}	17.740	18.338	18.662	17.788	18.910	27.851	16.998	16.446	16.719	18.069	18.034	16.696
		F_{OAE}	3.191	0.656	1.405	4.291	2.010	12.139	5.174	2.737	5.723	3.924	4.283	4.859
		F_{EO}	0.196	0.157	0.141	0.228	0.174	0.685	0.281	0.173	0.288	0.209	0.240	0.246
	Intersection	F_{MEO}	11.785	18.146	14.840	14.116	12.940	23.975	11.313	16.240	12.729	10.948	13.399	9.441
		F_{DP}	20.192	17.674	19.309	23.135	18.594	29.625	22.394	19.583	21.935	18.674	23.584	17.906
		F_{OAE}	3.419	4.233	3.638	4.263	4.020	5.166	3.479	3.133	4.945	3.388	3.885	3.667
		F_{EO}	0.251	0.312	0.256	0.329	0.232	0.678	0.305	0.307	0.285	0.225	0.314	0.232
Utility(%)	-	AUC	0.978	0.973	0.982	0.979	0.982	0.933	0.978	0.975	0.979	0.980	0.982	0.983
		ACC	0.920	0.862	0.895	0.928	0.916	0.832	0.921	0.849	0.921	0.920	0.930	0.933
		AP	0.978	0.977	0.984	0.978	0.984	0.915	0.979	0.978	0.978	0.979	0.981	0.984
		EER	0.070	0.088	0.075	0.066	0.064	0.141	0.076	0.087	0.074	0.070	0.065	0.066
		FPR	0.034	0.008	0.009	0.042	0.018	0.116	0.054	0.004	0.055	0.037	0.040	0.051

Table D.8. *Detailed fairness and utility evaluation results on a training subset with the ratio of real vs fake is 10:1.*

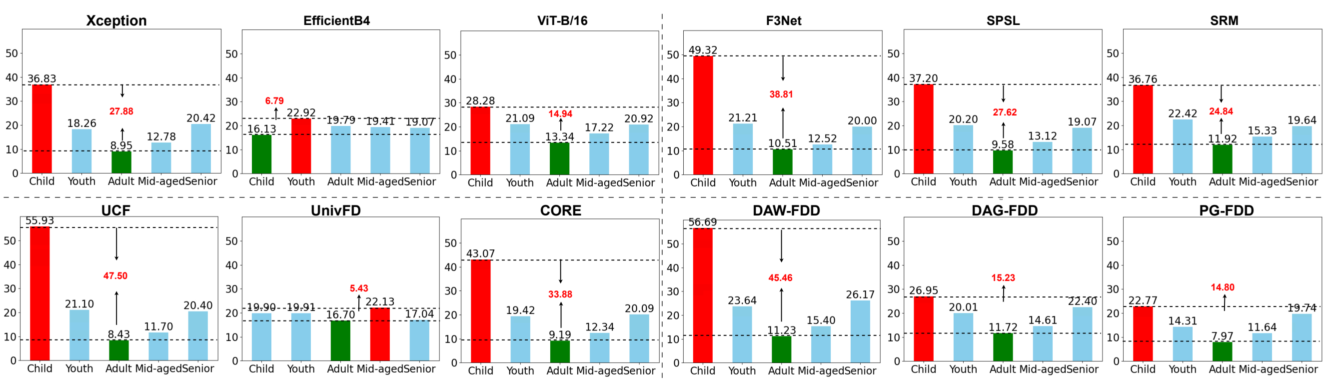

Figure D.1. *FPR(%) of each age subgroup. The subgroup with the highest FPR score is highlighted in red, while the subgroup with the lowest FPR score is shown in green.*

Method	Fairness																Utiliy				
	Skin Tone				Gender				Age				Intersection				-				
	F_{MEO}	F_{DP}	F_{OAE}	F_{EO}	F_{MEO}	F_{DP}	F_{OAE}	F_{EO}	F_{MEO}	F_{DP}	F_{OAE}	F_{EO}	F_{MEO}	F_{DP}	F_{OAE}	F_{EO}	AUC	ACC	AP	EER	FPR
EfficientB4	5.385	1.725	1.487	5.863	8.300	**6.184**	4.377	11.062	6.796	11.849	2.856	10.300	17.586	**8.607**	8.461	25.114	98.611	94.203	99.542	6.689	20.066
SPSL	4.411	1.827	1.037	4.534	8.055	9.379	1.135	9.789	27.614	11.232	7.270	40.943	10.379	13.259	2.464	21.679	98.747	96.346	99.356	4.371	13.661
UnivFD	4.503	1.19	1.622	5.408	2.577	8.556	2.748	5.536	5.436	15.249	3.793	14.148	6.119	14.026	6.287	20.255	98.192	93.651	99.400	7.633	18.550
PG-FDD	3.190	1.252	1.071	3.702	6.465	9.746	0.882	9.115	14.804	**10.467**	5.009	29.585	9.578	14.697	3.062	18.348	99.172	96.174	99.694	4.961	10.971
CLIP+MLP	**0.419**	**0.938**	**0.227**	**0.591**	**0.506**	8.658	**0.334**	**1.021**	**0.765**	14.473	**0.395**	**1.802**	**1.973**	13.992	**1.000**	**4.302**	**99.973**	**99.290**	**99.991**	**0.793**	**1.171**

Table D.9. *Fairness and utility performance of CLIP+MLP compared to representative detectors on the AI-Face dataset, highlighting the potential of foundation models for bias mitigation.*

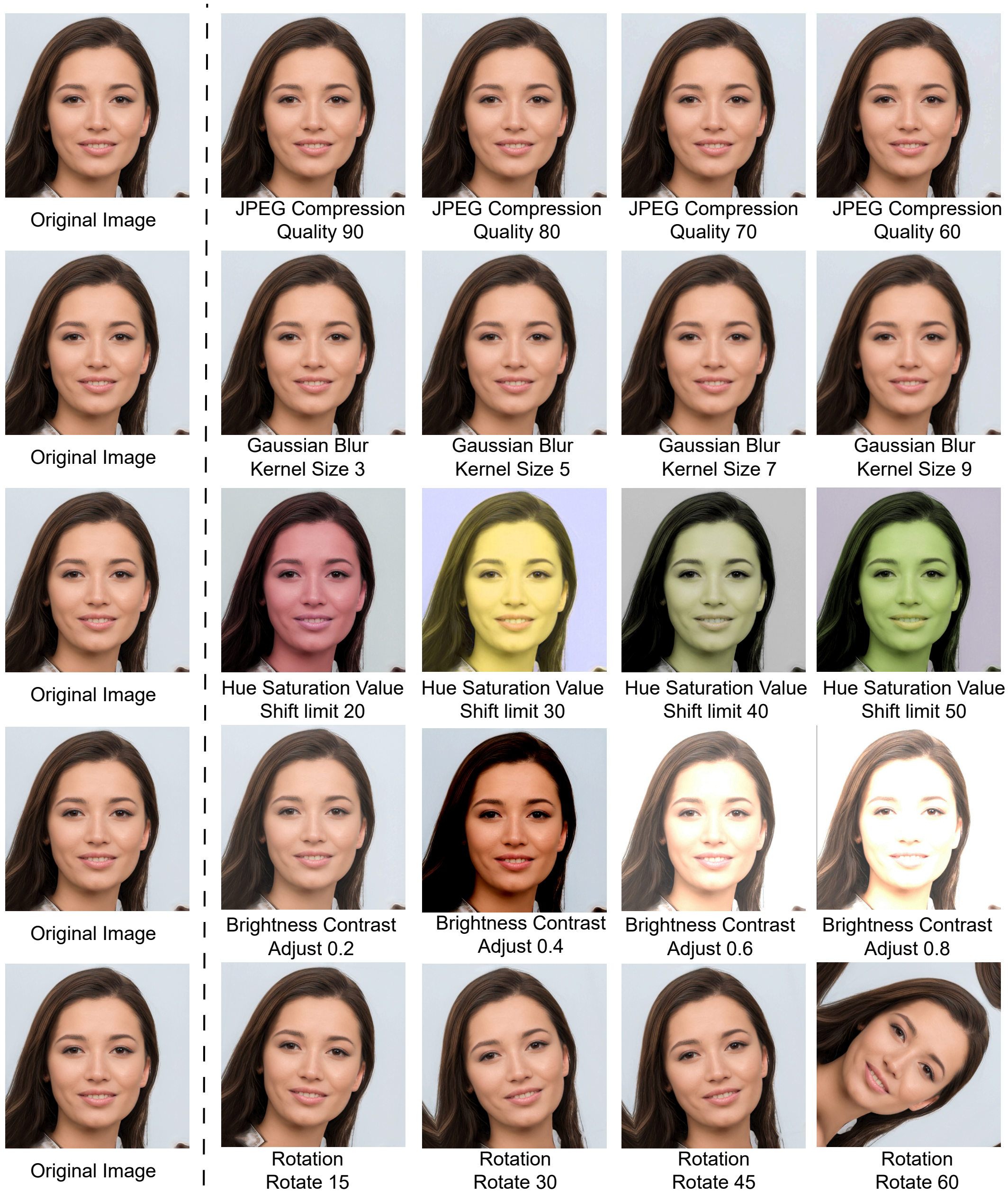

Figure D.2. *Visualization of the image after different post-processing.*

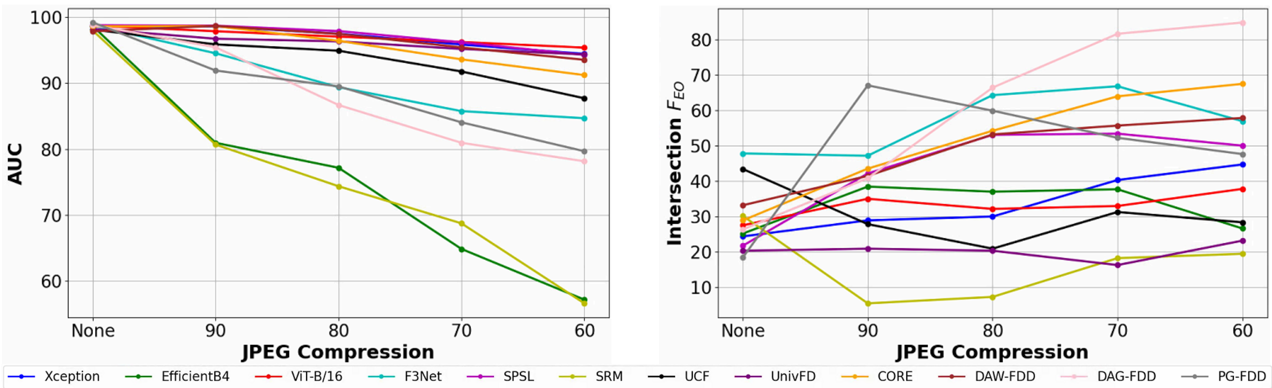

Figure D.3. *Robustness analysis in terms of utility and fairness under varying degrees of JPEG compression.*

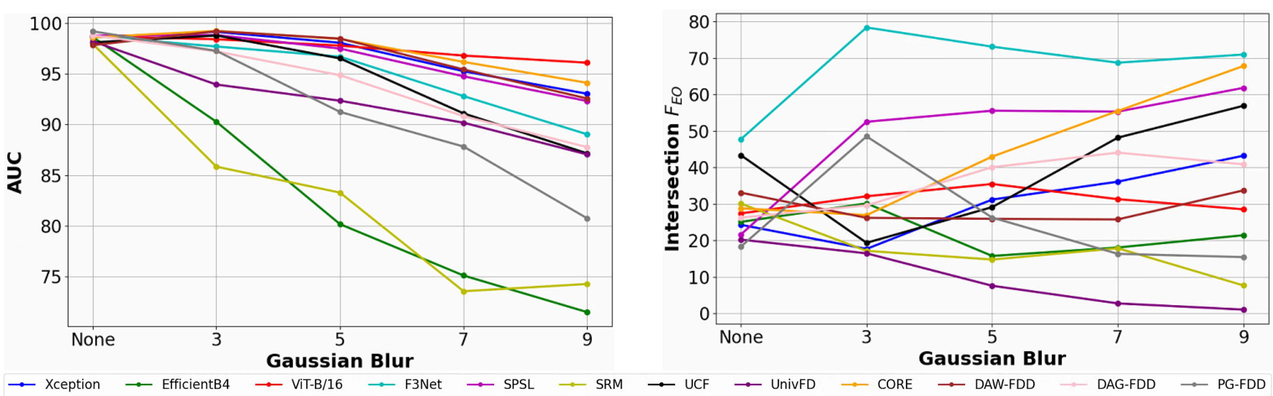

Figure D.4. *Robustness analysis in terms of utility and fairness under varying kernel sizes of Gaussian Blur.*

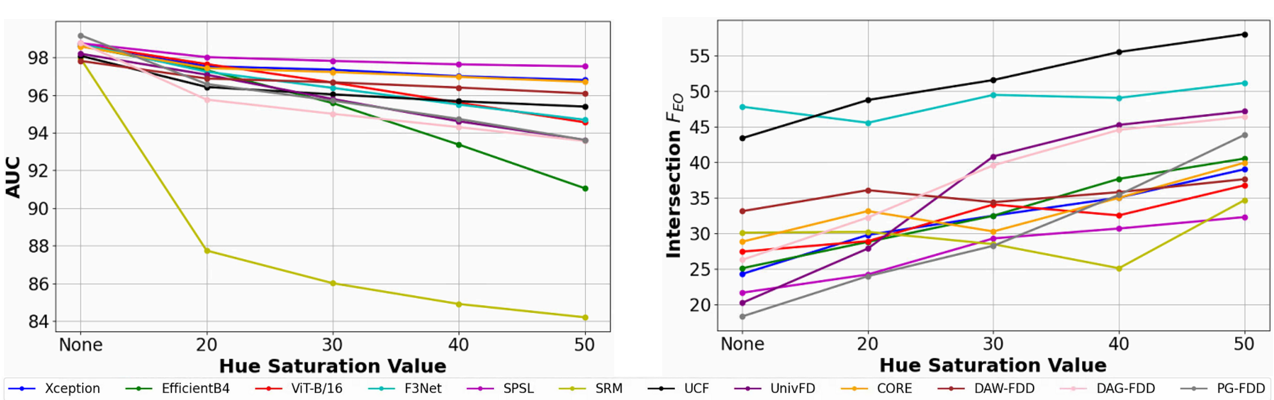

Figure D.5. *Robustness analysis in terms of utility and fairness under varying degrees of Hue Saturation Value.*

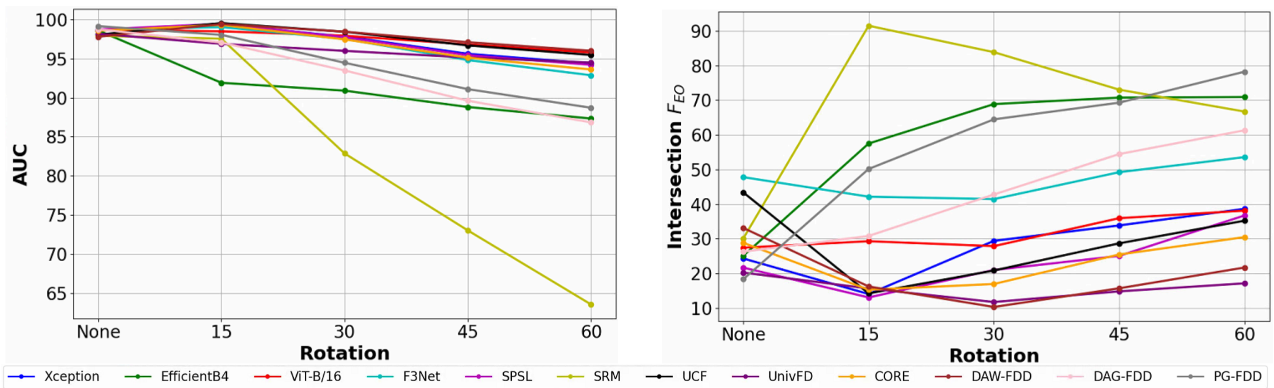

Figure D.6. *Robustness analysis in terms of utility and fairness under varying degrees of Rotations.*

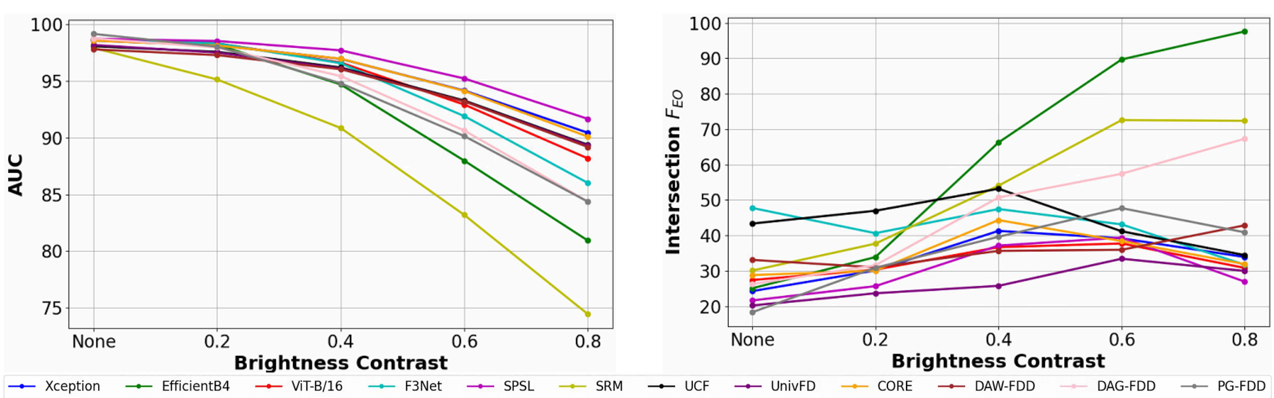

Figure D.7. *Robustness analysis in terms of utility and fairness under varying degrees of Brightness Contrast.*

E. Datasheet for AI-Face

In this section, we present a DataSheet [118] for AI-Face.

E.1. Motivation For Dataset Creation

- **Why is the dataset created?** For researchers to evaluate the fairness of AI face detection models or to train fairer models. Please see Section 2 'Background and Motivation' in the submitted manuscript.
- **Has the dataset been used already?** Yes. Our fairness benchmark is based on this dataset.
- **What (other) tasks could the dataset be used for?** Could be used as training data for generative methods attribution task.

E.2. Data Composition

- **What are the instances?** The instances that we consider in this work are real face images and AI-generated face images from public datasets.
- **How many instances are there?** We include 1,646,545 face images from public datasets. Please see Table B.1 for details.
- **What data does each instance consist of?** Each instance consists of an image.
- **Is there a label or target associated with each instance?** Each image is associated with gender annotation, age annotation, skin tone annotation, intersectional attribute (gender and skin tone) annotation, and target label (fake or real).
- **Is any information missing from individual instances?** No.
- **Are relationships between individual instances made explicit?** Not applicable – we do not study the relationship between each image.
- **Does the dataset contain all possible instances or is it a sample?** Contains all instances our curation pipeline collected. Since the current dataset does not cover all available images online, there is a high probability more instances can be collected in the future.
- **Are there recommended data splits (*e.g.*, training, development/validation, testing)?** For detector development and training, the dataset can be split as 6:2:2.
- **Are there any errors, sources of noise, or redundancies in the dataset? If so, please provide a description.** Yes. Despite our extensive efforts to mitigate the bias that may introduced by the automated annotator and reduce demographic label noise, there may still be mislabeled instances. Given the dataset's size of over 1 million images and most are generated face images, it is impractical for humans to manually check and correct each image individually.
- **Is the dataset self-contained, or does it link to or otherwise rely on external resources (e.g., websites, tweets, other datasets)?** The dataset is self-contained.

E.3. Collection Process

- **What mechanisms or procedures were used to collect the data?** We build our AI-Face dataset by collecting and integrating public AI-generated face images sourced from academic publications, GitHub repositories, and commercial tools. Please see 'Data Collection' in Section 3.1
- **How was the data associated with each instance acquired? Was the data directly observable (*e.g.*, raw text, movie ratings), reported by subjects (*e.g.*, survey responses), or indirectly inferred/derived from other data?** The data can be acquired after our verification of user submitted and signed EULA.
- **If the dataset is a sample from a larger set, what was the sampling strategy (*e.g.*, deterministic, probabilistic with specific sampling probabilities)?** Not applicable. We did not sample data from a larger set. But we use RetinaFace [66] for detecting and cropping faces to ensure each image only contains one face.
- **Over what timeframe was the data collected? Does this timeframe match the creation timeframe of the data associated with the instances (*e.g.*, recent crawl of old news articles)? If not, please describe the timeframe in which the data associated with the instances was created.** The data was collected from February 2024 to April 2024, even though the data were originally released before this time. Please refer to the cited papers in Table B.1 for specific original data released time.

E.4. Data Processing

- **Was any preprocessing/cleaning/labeling of the data done (*e.g.*, discretization or bucketing, tokenization, part-of-speech tagging, SIFT feature extraction, removal of instances, processing of missing values)?** Yes. We discussed in 'Data Collection' in Section 3.1.

- **Was the 'raw' data saved in addition to the preprocessed/cleaned/labeled data (*e.g.*, to support unanticipated future uses)? If so, please provide a link or other access point to the 'raw' data.** The 'raw' data can be acquired through the original data publisher. Please see the cited papers in Table B.1.
- **Is the software used to preprocess/clean/label the instances available? If so, please provide a link or other access point.** Yes. We use RetinaFace [66] for detecting and cropping faces to ensure each image only contains one face. Demographic annotations are given by our annotator, see 'Annotation Generation' in Section 3.2. Our annotator code will not be released considering the ethical guidelines.
- **Does this dataset collection/processing procedure achieve the motivation for creating the dataset stated in the first section of this datasheet? If not, what are the limitations?** Yes. The dataset does allow for the study of our goal, as it covers comprehensive generation methods, demographic annotations for evaluating current detectors and training fairer detectors.

E.5. Dataset Distribution

- **How will the dataset be distributed?** We distribute all the data as well as CSV files that formatted all annotations of images under the CC BY-NC-ND 4.0 license and strictly for research purposes.
- **When will the dataset be released/first distributed? What license (if any) is it distributed under?** The dataset will be released following the paper's acceptance, and it will be under the permissible CC BY-NC-ND 4.0 license for research-based use only. Users can access our dataset by submitting an EULA.
- **Are there any copyrights on the data?** We believe our use is 'fair use' since all data in our dataset is collected from public datasets.
- **Are there any fees or access restrictions?** No.

E.6. Dataset Maintenance

- **Who is supporting/hosting/maintaining the dataset?** The first author of this paper.
- **Will the dataset be updated? If so, how often and by whom?** We do not plan to update it at this time.
- **Is there a repository to link to any/all papers/systems that use this dataset?** Our fairness benchmark uses this dataset, a brief instruction of how to use this dataset and the code of fairness benchmark is on `https://anonymous.4open.science/r/AI_Face_FairnessBench-E417`.
- **If others want to extend/augment/build on this dataset, is there a mechanism for them to do so?** Not at this time.

E.7. Legal and Ethical Considerations

- **Were any ethical review processes conducted (*e.g.*, by an institutional review board)?** No official processes were done since all data in our dataset were collected from the existing public datasets.
- **Does the dataset contain data that might be considered confidential?** No. We only use data from public datasets.
- **Does the dataset contain data that, if viewed directly, might be offensive, insulting, threatening, or might otherwise cause anxiety? If so, please describe why** No. It is a face image dataset, we have not seen any instance of offensive or abusive content.
- **Does the dataset relate to people?** Yes. It is a face image dataset containing real face images and AI-generated face images.
- **Does the dataset identify any subpopulations (*e.g.*, by age, gender)?** Yes, through demographic annotations.
- **Is it possible to identify individuals (*i.e.*, one or more natural persons), either directly or indirectly (*i.e.*, in combination with other data) from the dataset?** Yes. It is a face image dataset. The age, gender, and skin tone can be identified through the face image, also through the demographic annotation we provide. All of the images that we use are from publicly available data.

E.8. Author Statement and Confirmation of Data License

The authors of this work declare that the dataset described and provided has been collected, processed, and made available with full adherence to all applicable ethical guidelines and regulations. We accept full responsibility for any violations of rights or ethical guidelines that may arise from the use of this dataset. We also confirm that the dataset is released under the CC BY-NC-ND 4.0 license, permitting sharing and downloading of the work in any medium, provided the original author is credited, and it is used non-commercially with no derivative works created.

E.9. Annotator Agreement

Annotator Agreement

Project Title: AI-Generated Face Image Annotation

Date: 9/15/2024

---

1. Introduction

This agreement establishes the guidelines and procedures for annotating AI-generated face images. The primary objective of this task is to ensure the collection of consistent and accurate annotations for gender and age classifications, which will **serve as ground truth for the experiment evaluation of annotation quality.**

2. Participants

Three annotators will participate in this project:

- Annotator A: [xxxx]
- Annotator B: [xxxx]
- Annotator C: [xxxx]

3. Objective

Annotators are required to:

- Review each provided AI-generated face image.
- Assign appropriate labels for **gender** and **age** according to the guidelines specified in this agreement.
- Ensure consistency and accuracy in annotations across all images.

4. Annotation Guidelines

4.1. Gender Annotation

Sex at birth (male and female), an individual whose gender identity aligns with those typically associated with the biological sex assigned to them at birth.

- **Female (0)**: Images that display characteristics biologically associated with females, including biological features such as a more rounded face, wider hips, and the absence of prominent facial hair. Visually, females often have softer facial features, fuller lips, and longer hairstyles, though hair length may vary. Females may also show more pronounced cheekbones and smaller noses compared to males.

- **Male (1)**: Images that display characteristics biologically associated with males.including biological features such as a more prominent Adam's apple, and facial hair (e.g., beard or mustache). Visually, males often have a more angular jawline, thicker eyebrows, and shorter hairstyles, although hairstyle may vary.

Note: If the gender is ambiguous, please select the gender that the facial features most closely resemble based on traditional attributes.

Real images are used as example images to educate human annotators to distinguish demographic attributes..

Demographic Annotation	Examples			
Female: 0		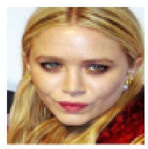	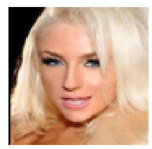	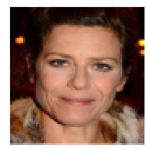
Male: 1				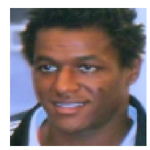

4.2. Age Annotation

- **Child (0)**: Individuals appearing to be approximately 0-14 years old.
- **Youth (1)**: Individuals appearing to be approximately 15-24 years old.
- **Adult (2)**: Individuals appearing to be approximately 25-44 years old.
- **Middle-age Adult (3)**: Individuals appearing to be approximately 45-64 years old.
- **Senior (4)**: Individuals appearing to be 65+ years old.

Guidelines:

- Consider facial features such as skin elasticity, wrinkles, and other age-indicating characteristics.
- If uncertain, use your best judgment based on the visual cues present.

Demographic Annotation	Examples			
Child (0-14): 0	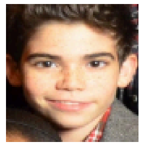		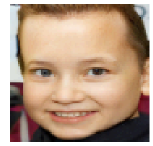	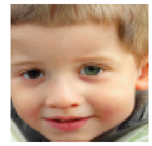
Youth (15-24): 1		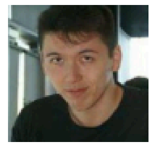		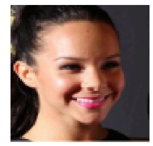
Adult (25-44): 2	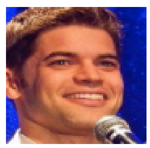	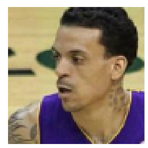	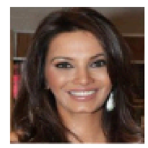	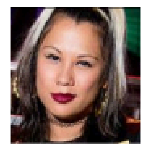
Middle-age Adult (45-64): 3			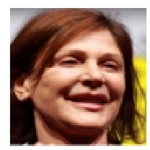	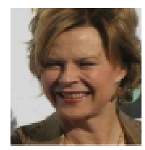
Senior (65+): 4	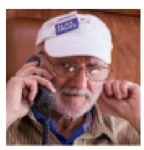			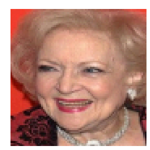

4. Annotation Procedure

1. **Review Images**: Each annotator will receive the same set of AI-generated face images.
2. **Independent Work**: Annotations should be done independently to avoid bias.
3. **Data Entry**: For each image, record the assigned labels for gender and age on the CSV files provided.

5. Confidentiality and Data Security

- All images and annotations are confidential.
- Annotators must not share or distribute images or annotation data outside of this project.
- All data should be stored securely, and any physical documents should be kept in a safe location.

6. Code of Conduct

- **Impartiality**: Annotators must remain objective and base annotations solely on the guidelines provided.
- **Respect**: Treat all content with respect and professionalism.
- **Compliance**: Adhere strictly to the guidelines to ensure data consistency and integrity.

7. Conflict Resolution

- Conflicts will be resolved by majority vote.
- If all three annotators have different annotations (no majority), three annotators will discuss and decide the final annotation.

8. Agreement Duration

This agreement is valid for the duration of the annotation project, starting from 9/15/2024 to 9/22/2024.

9. Acknowledgment

By signing below, you acknowledge that you have read, understood, and agree to abide by the terms and guidelines outlined in this agreement. All annotators confirm that they are comfortable labeling AI-generated face images and understand that the images do not represent real individuals.

Annotator A

Name: _______________ Signature: _________________ Date: ________________

Annotator B

Name: _______________ Signature: _________________ Date: ________________

Annotator C

Name:_______________ Signature: _________________ Date: ________________